



# Mechanical properties of cell sheets and spheroids: the link between single cells and complex tissues

Yuri M. Efremov<sup>1,2</sup> · Irina M. Zurina<sup>1,3</sup> · Viktoria S. Presniakova<sup>1</sup> · Nastasia V. Kosheleva<sup>1,2,3</sup> · Denis V. Butnaru<sup>4</sup> · Andrey A. Svistunov<sup>5</sup> · Yury A. Rochev<sup>1,6</sup> · Peter S. Timashev<sup>1,2,7,8</sup>

Received: 23 June 2021 / Accepted: 5 July 2021 / Published online: 13 July 2021

© International Union for Pure and Applied Biophysics (IUPAB) and Springer-Verlag GmbH Germany, part of Springer Nature 2021

## Abstract

Cell aggregates, including sheets and spheroids, represent a simple yet powerful model system to study both biochemical and biophysical intercellular interactions. However, it is becoming evident that, although the mechanical properties and behavior of multicellular structures share some similarities with individual cells, yet distinct differences are observed in some principal aspects. The description of mechanical phenomena at the level of multicellular model systems is a necessary step for understanding tissue mechanics and its fundamental principles in health and disease. Both cell sheets and spheroids are used in tissue engineering, and the modulation of mechanical properties of cell constructs is a promising tool for regenerative medicine. Here, we review the data on mechanical characterization of cell sheets and spheroids, focusing both on advances in the measurement techniques and current understanding of the subject. The reviewed material suggest that interplay between the ECM, intercellular junctions, and cellular contractility determines the behavior and mechanical properties of the cell aggregates.

**Keywords** Cell aggregates · Cell sheets · Cell spheroids · Mechanical properties · Mechanobiology

## Introduction

Along with biochemical causes, the mechanical stresses applied to cells and tissues and their intrinsic mechanical properties that form the basis of their mechanical responses are fundamental factors that determine cellular behavior and tissue functionality (Engler et al. 2006; Lecuit and Lenne 2007; Jansen et al. 2015; Vogel 2018; Gómez-González et al. 2020). The growing realization of the importance of mechanical properties and mechanical interactions has driven collaboration between the fields of material engineering in the fields of cell and tissue biology, tissue engineering, and regenerative medicine (Kasza et al. 2007; Smith 2010; Gonzalez-Rodriguez et al. 2012; Jansen et al. 2015; Xi et al. 2019; Guimarães et al. 2020). Although many previous works have been devoted to the study of mechanical properties at the level of single cells (Kasza et al. 2007; Basoli et al. 2018; Narasimhan et al. 2020), most cells within the human body exist as part of a tissue and thereby interact with neighboring cells and extracellular matrix (ECM) components to establish a unique 3-D organization (Knight and Przyborski 2015; Xi et al. 2019; Guimarães et al. 2020). These interactions form a complex communication network of biochemical and mechanical signals that are critical for normal cell physiology

✉ Yuri M. Efremov  
yu.efremov@gmail.com

<sup>1</sup> Institute for Regenerative Medicine, Sechenov First Moscow State Medical University (Sechenov University), 119991 8-2 Trubetskaya St, Moscow, Russia

<sup>2</sup> World-Class Research Center “Digital Biodesign and Personalized Healthcare”, Sechenov University, Moscow 119991, Russia

<sup>3</sup> FSBSI Institute of General Pathology and Pathophysiology, 125315, 8 Baltiyskaya St, Moscow, Russia

<sup>4</sup> Institute for Urology and Reproductive Health, Sechenov University, Moscow, Russia

<sup>5</sup> Sechenov First Moscow State Medical University (Sechenov University), 119991, 8-2 Trubetskaya St, Moscow, Russia

<sup>6</sup> Centre for Research in Medical Devices (CÚRAM), National University of Ireland Galway, GalwayH91 W2TY, Ireland

<sup>7</sup> Department of Polymers and Composites, N.N. Semenov Institute of Chemical Physics, 119991 4 Kosygin St, Moscow, Russia

<sup>8</sup> Chemistry Department, Lomonosov Moscow State University, Leninskiye Gory 1–3, Moscow 119991, Russia

(Lin and Chang 2008). While such interactions could (necessarily) not be recreated at the single-cell level, often-times, measurements at the tissue level are limited by both the complexities of tissue structures and the capabilities of measurement and imaging techniques.

The multicellular structures obtained *in vitro* can be seen as an intermediate level of organization between single cells and the complex tissue structures presented *in vivo*. There is a growing trend to use multicellular structures for both fundamental studies and practical applications (Shen et al. 2021; Imashiro and Shimizu 2021). These structures, which include cell sheets and spheroids, possess such advantageous properties as pre-formed intercellular junctions and pre-synthesized ECM, which together result in a more relevant platform with the formation of a microenvironment closer to native tissues and thus favoring cell survival, differentiation, and integration with host tissues. Both spheroids and cell sheets can be used in tissue engineering as self-sustainable scaffold-free constructs (Yoshikawa et al. 2018; Venugopal et al. 2020; Krasina et al. 2020; Hsu et al. 2021), bioprinting material (Bakirci et al. 2017; Burdis and Kelly 2021; Daly et al. 2021), or in combination with various scaffolds (Baptista et al. 2018; Zurina et al. 2020b). Additionally, tissue engineering techniques based on the use of cell aggregates may offer advantages for technologies involving *in vitro* food production (Bhat and Fayaz 2011; Bhat et al. 2015).

Cell sheets and cell spheroids are the simplest models of cell aggregates, which both possess intercellular interactions with paracrine signaling while also partially recreating the structural complexity of the native tissues containing ECM. Cell sheets have been described as two-dimensional (2D) self-organized multicellular patches (Kobayashi et al. 2019a), and spheroids as self-organized 3D spherical cell aggregates (Cui et al. 2017). Many previous studies have emphasized the biological significance of such structures (Lin and Chang 2008; Cui et al. 2017; Zurina et al. 2020b; Shen et al. 2021), but less is known about their mechanical properties (Zhang et al. 2012). It is our contention that a proper understanding the mechanical behavior of these multicellular model systems is a necessary step for making progress in the field of tissue mechanics and determining its fundamental principles. These principles are fundamentally related to the mechanisms of new tissue formation, regeneration, and disease. At the same time, there are purely practical reasons coming from the field of tissue engineering that are related to predictive modeling and rational design of cell-based biomaterials. The use of cell sheets both alone and in conjunction with biomaterials can create specific microenvironments that are able to promote new tissue morphogenesis. There is a need for targeted adjustment of the cell sheet mechanical properties in order to improve the ease of handling and promote their practical application in tissue/organ repair and regeneration. Cell aggregates hold the potential to be widely utilized as

implantable therapeutics and as building blocks for the construction of complex tissues of arbitrary structure via bioprinting (Norotte et al. 2009; Shafiee et al. 2017; Daly et al. 2021). Mechanical interactions affect cell aggregate formation, viability, and fusion processes, and thus mechanical tuning is a promising pathway for augmentation of such processes.

In this review, we first briefly overview techniques that are used for the production of cell sheets and spheroids. We then provide information on both well-established, and recent techniques, used for the mechanical characterization of multicellular aggregates. Current data on mechanical properties of the cell sheets and spheroids are presented in respective sections. Relations between mechanical properties of single cells, extracellular matrix (ECM), and tissues are further discussed. In the final section, we summarize the reviewed material and address the open questions of the field.

## Experimental techniques

### Methods of acquisition of cell sheets and spheroids

Methods for generating cell sheets and spheroids have been under continuous development in recent years (Fig. 1). The interested reader is directed to recent reviews of this area that focus on cell sheets (Kobayashi et al. 2019a; Zurina et al. 2020b; Imashiro and Shimizu 2021) and spheroids (Cui et al. 2017; Białkowska et al. 2020; Liu et al. 2021). Here, we introduce key techniques in both areas. It should be noted that the specific details of a particular method used for the generation of a cell aggregate can greatly affect its composition and mechanical properties, with these sensitivities described in more detail in subsequent sections of this Review.

Cell sheet engineering is a technology that has benefited greatly from the development of stimuli-responsive polymers, mainly thermoresponsive polymers. For example, thermoresponsive polymer poly(N-isopropylacrylamide) (PNIPAAm) undergoes a phase transition at its lower critical solution temperature (LCST), which is 32 °C (Nagase et al. 2018). The polymer film surface is hydrophobic above LCST and transforms to hydrophilic as the temperature drops below LCST (Akiyama et al. 2004). Thus, cells attach to PNIPAAm-coated surfaces and proliferate to form cell sheets at 37 °C (normal culture conditions), which then can be detached by reducing the temperature below the LCST with the ECM remaining on the basal surfaces of cell sheets (Nagase et al. 2018; Kobayashi et al. 2019a). Thermoresponsive surfaces can be prepared by irradiation, grafting, and coating techniques (Dzhoyashvili et al. 2016) or through physical adsorption (Tang and Okano 2014; Healy et al. 2017a). Thermoresponsive polymers can also be used as hydrogels (Kim et al. 2013), physical gel (Healy et al. 2017b) or

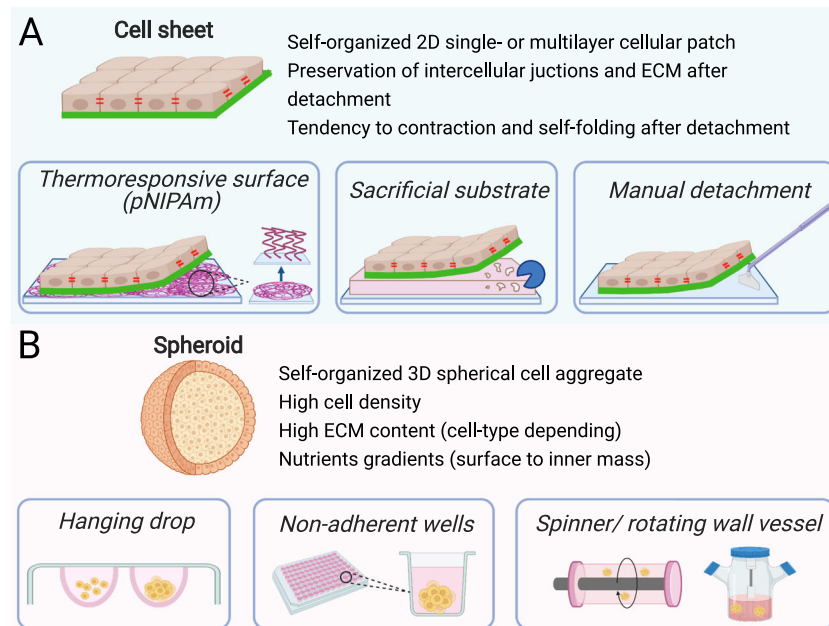


**Fig. 1** Commonly used techniques to generate cell sheets (A) and spheroids (B). (A) Generation of cell sheets: temperature-responsive surfaces allow detachment of contiguous cell sheet upon reducing temperature (PNIPAAm: Poly(N-isopropylacrylamide)); sacrificial substrate which can be dissolved with a specific ferment to release a cell sheet growing on top of it; manual detachment with cell scraper is

possible for some types of cell sheets. (B) Generation of spheroids: in the hanging drop technique, cells are aggregated by gravitational force; low-attachment surfaces of wells or micro-wells promote the aggregation and self-organization of cells; spinner flask and rotating wall vessel simulate cell aggregation and compaction in suspension

electrospun fibers (Young et al. 2019). The approach of using thermoresponsive culture vessels remains the most popular due to the fact that pNIPAm-grafted Petri dishes are commercially available (Tang and Okano 2014). Other methods for obtaining cell sheets include mechanical detachment using cell scrapers (Okuda et al. 2017; You et al. 2020), ultrasonic vibration (Imashiro et al. 2020), use of ECM protein-covered surfaces with subsequent application of specific degradative enzymes (Kamao et al. 2017; Fujita et al. 2019), and magnetic force procedures (Silva et al. 2020). More complex methods for obtaining 3D structures based on a combination of micro-stereolithography (to produce matrices of desirable shape), surface modification with biocompatible golden particles, and electrochemical cell detachment have also been described (Kobayashi et al. 2019b).

Cell spheroids have been widely used for the investigation of tumorigenesis, intracellular interactions, cell differentiation and metabolism, the evaluation of toxicity and efficacy of potential drugs, and also of cellular bioprinting (Blakely et al. 2013; Białkowska et al. 2020; Zurina et al. 2020a; Gorkun et al. 2021). Formation of spheroids is achieved using either scaffold-free systems, such as hanging drops, low adherence substrates, microwells, magnetic force levitation, rotating bioreactors, or scaffold-based systems, such as hydrogels and microfluidic chambers (Białkowska et al. 2020; Shen et al. 2021). The hanging drop method was invented by Ross Granville Harrison at Yale in 1910 (Millet and Gillette 2012). The principle behind the method is the

interaction between surface tension and the gravity field of the hanging drop that promotes cell aggregation into a spheroid. Commonly, the drops are just placed onto the underside of a Petri dish lid. The method is relatively simple and does not require any additional equipment, yet it requires significant manual input. The volume of drops is small (20–30  $\mu\text{L}$ ) with a low media-to-cell ratio (Białkowska et al. 2020). Besides, not all cell types can form compact dense spheroids in hanging drops, and intercellular interactions might be hampered compared to 2D monolayers (Schmal et al. 2016). The method of low adherence substrates utilizes the fact that cells seeded on such substrate cannot attach to its surface; instead, they aggregate with each other to form spheroids. Chemical or topological modification of the substrate can be performed to make it low-adherent. Agarose, poly(2-hydroxyethyl methacrylate) (polyHEMA), poly(ethylene glycol) (PEG), and polyvinyl alcohol (PVA) are all used as low-adherent coatings (Cui et al. 2017). While spheroids from different cell types can be formed relatively easily, the control of aggregates' size and shape is difficult to achieve (Kim et al. 2018; Li et al. 2019; Liu et al. 2021). The problem is addressed by modifying this technique, which is the use of wells or microwells with low-adherence surfaces. Commercially available multi-well microplates (spheroid microplates) with ultra-low attachment surfaces have been used for high reproducibility (Locquet et al. 2021). The microwells are generally formed at the bottom of a larger compartment that is filled with a large volume of culture medium and cells. Under the action of

gravity, the cells settle from the suspension into the microwells and form one spheroid per well (Zurina et al. 2018; Chao et al. 2020). However, there is a probability of uncontrolled transition of spheroids between the microwells and subsequent fusion, for example, during medium change. Cell aggregation can also be stimulated by ultrasound (Liu et al. 2007) or magnetic levitation via an external magnetic field acting on cells pre-loaded with magnetic nanoparticles or located in a paramagnetic medium, for example, containing gadolinium salts (Parfenov et al. 2020; Labusca et al. 2021). Different types of agitation bioreactors are used for the spheroid generation, such as spinner flasks, rotary shakers, and microgravity bioreactors (Hammond and Hammond 2001; Zhang et al. 2015). The proper adjustment of cultivation parameters is required, sometimes dependent on spheroid formation stage (Liu et al. 2021).

Biological polymers, such as collagen or Matrigel, and non-biological polymeric scaffolds are also used for spheroid formation (Cui et al. 2017). They both provide physical support, biomechanical and biochemical signals for cells to attach and reorganize into 3D structures. Microfluidics can be used to encapsulate cells in hydrogels, such as alginates or polyethylene glycol (PEG), and shorten the production time of spheroids (Shen et al. 2021). Overall, scaffold-based techniques allow the formation of 3D cell structures with high complexity, yet require more time for individual fabrication steps and optimization of conditions for proper spheroid organization.

## Techniques for mechanical characterization of cell sheets and spheroids

Specific size and structural features of the cell aggregates imply some limitations for the use of mechanical measurement techniques (Zhang et al. 2012). Nevertheless, a wide range of such techniques are currently available, and these can be divided into techniques that measure either global (macroscale to microscale) or local (microscale to nanoscale), and either bulk or surface properties (Fig. 2). Common to all experiments with cellular samples, the measurements are generally performed in an appropriate liquid medium and preferably with temperature control to maintain cell viability (Sunyer et al. 2009; Arroyave et al. 2015).

The bulk techniques deform the object as a whole, allowing bulk mechanical properties to be measured. In the case of cell sheets, a uniaxial tensile test is an example of such a technique (Harris et al. 2013; Uesugi et al. 2013; Backman et al. 2017b) (Fig. 3D, E), while for the spheroids, it is a uniaxial parallel plate compression (Norotte et al. 2008; Brodland et al. 2009). A relationship between global stress and strain is established in both types of tests to estimate the bulk properties. The tensile test requires a firm attachment of the sample edges, which is a technical problem for fragile sample like cell sheets where clamping forces, and usage of pins or staples, can

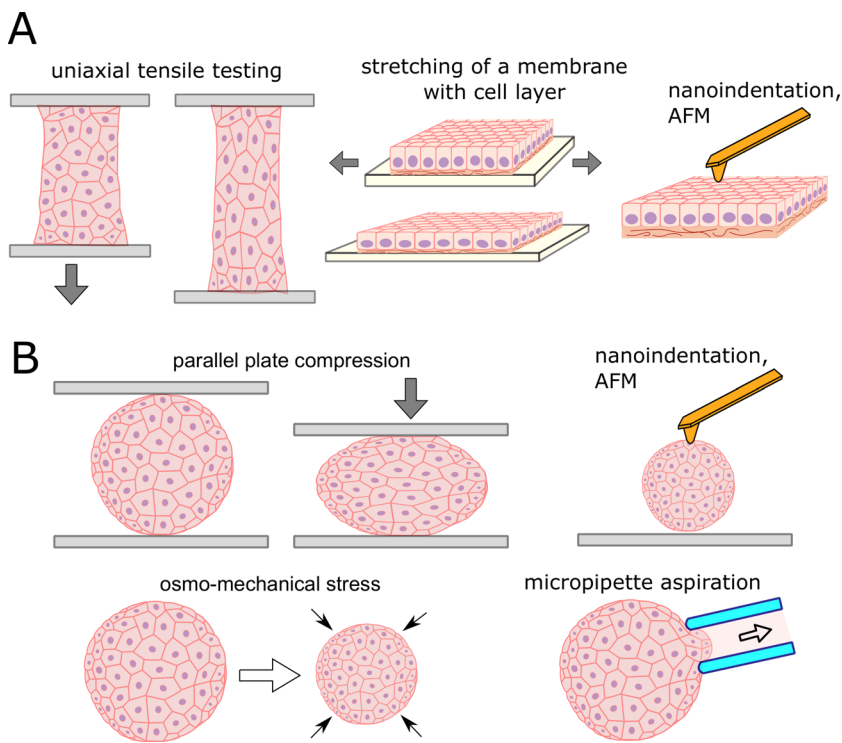
damage or tear of the sample (Uesugi et al. 2013). The attachment is currently achieved by the use of specially designed fixtures (Uesugi et al. 2013), glue (Backman et al. 2017b), or by natural attachment of growing cells to specially designed cell-adhesive rods (Harris et al. 2013). The self-attachable fixtures were developed, consisting of arrays of non-penetrating hooks and utilizing the fact that cell sheet contracts and curls around the hooks after detachment (Uesugi et al. 2013). The deflecting rod (e.g., metal cantilever or glass capillary) with a calibrated spring constant might be used both as an attachment fixture and as a force sensor in tensile tests (Harris et al. 2013; Jaiswal et al. 2017). Otherwise, high-precision force sensors are required to register low forces during the extension process (Backman et al. 2017b).

The mechanical properties of the cell sheet might be measured with a soft elastomer membrane used as a substrate for its growth (Dassow et al. 2013; Sorba et al. 2019). By measuring the mechanical behavior of the membrane with and without cells grown on it, the mechanical parameters of the cells can be inferred. The membrane, however, should be very soft (like cells themselves) for sensitive measurements. Uniaxial (Sorba et al. 2019) and equibiaxial (Dassow et al. 2013) stretching is possible with such setups.

The compression test is performed between two parallel plates with controllable deformation and force (Fig. 4C). Compression of the spheroids does not require special means for the sample attachment, but a good resolution in forces (nN range) and displacements (< 0.1 um) is required. For example, special planar AFM macro-probes were designed to allow spheroid compression and utilize the high precision of an AFM instrument (Andolfi et al. 2019). The tracing of the spheroid shape during the compression can be performed to allow the use of more advanced mechanical models (Norotte et al. 2008; Shafiee et al. 2017). Global isotropic loading was also achieved by the application of osmo-mechanical stress (Montel et al. 2011; Leroux et al. 2015). Another method consists of spheroid centrifugation, where mechanical properties can be determined by fitting the shape of an aggregate produced in response to the application of centrifugal force (Kalantarian et al. 2009).

While the above-mentioned methods evaluate the bulk sample properties, the measurement of local properties at different scales is also possible by using different techniques. The most popular technique for single-cell studies, but which can be extended to cell sheets and spheroids, is atomic force microscopy (AFM) (Kasas et al. 2018; Krieg et al. 2019; Efremov et al. 2020). AFM utilizes the mechanical interaction of a probe (sharp conical or dull spherical tip located at the end of a cantilever) with the sample surface (Binnig et al. 1986). The mechanical measurements are generally performed using the force spectroscopy mode of the AFM whereby the probe indents the surface of the sample (so-called nano-indentation experiments). By analyzing the force curves, which describe

**Fig. 2** Techniques to measure mechanical properties of cell sheets (A) and spheroids (B). (A) Global mechanical properties of cell sheets can be assessed with uniaxial tensile testing performed on cell sheets attached on two sides, and with stretching of a thin soft elastomeric membrane with attached cell sheet. AFM and nanoindentation can be applied to measure local mechanical properties on the surface of the cell sheet. (B) Spheroid can be compressed between two parallel plates, or osmo-mechanical stress can be applied for the global measurements, while local measurements can be performed with AFM, nanoindentation, and micropipette aspiration



the dependence of the applied force on the indentation depth, a local Young's modulus of a sample can be calculated. By making measurements at different points over the sample, the mechanical mapping can be performed with a high spatial resolution (Fig. 3G) (Efremov et al. 2019a). However, the method is limited by the surface region of the sample, which is the top cell layer in the case of the spheroids or cell sheets (Jorgenson et al. 2017; Zhu et al. 2021). An increase of the indentation depth and probe dimension, in principle, might allow for evaluation of the depth-dependent and bulk properties of the samples (Vyas et al. 2019). Specialized instruments, nanoindenters, might also be used with similar operating principles (Kosheleva et al. 2020; Ryu et al. 2021). For accurate measurements, the sample should be properly immobilized, for example, by partial embedding in agarose gel or attachment on polylysine-coated surfaces (Vyas et al. 2019; Kosheleva et al. 2020). For the immobilization of large organoids, 3D multi-functional mesoscale frameworks were recently developed to enclose an organoid in a controlled manner, allowing for accurate and repeated nanoindentation measurements (Ryu et al. 2021).

The micropipette aspiration technique has been applied to study the mechanical properties of single cells and cell aggregates (Guevorkian et al. 2010; Guevorkian and Maître 2017; González-Bermúdez et al. 2019). Deformation (aspiration) is induced by a negative pressure (suction) that is created with a hydrostatic system (Fig. 4F). A morphology change of a sample is recorded to analyze the deformation, which may be compared to numerical simulation to obtain mechanical

properties like Young's modulus or surface tension (González-Bermúdez et al. 2019). By varying the diameter of the micropipette, the bulk or local properties can be assessed (Guevorkian and Maître 2017).

Improvements in spatial resolution have paved the way for the application of elastography-based methods for multicellular constructs (Leroux et al. 2015; Larin and Sampson 2017; Jaiswal et al. 2019; Zhang et al. 2021). Elastography involves the visualization of the internal elasticity distribution based on ultrasound, magnetic resonance, or optical imaging and is generally divided into two main types: shear wave elastography and strain-imaging (Zaitsev et al. 2021). In shear wave elastography, the local shear modulus of a sample is determined by measuring the velocity of an applied shear wave, which travels faster through stiffer regions than through softer ones. High resolution in shear wave elastography is currently achieved with optical coherence tomography/elastography (OCT, OCE) and Brillouin microscopy (Conrad et al. 2019) with sub-cellular resolution being achieved with the state-of-art OCT systems (Mazlin et al. 2018; Hepburn et al. 2020). Brillouin light scattering is based on the interaction of light with spontaneous, thermally induced density fluctuations, which are also considered as microscopic acoustic waves, phonons (Prevedel et al. 2019). Both OCT/OCE and Brillouin microscopy techniques are label-free and allow 3D mapping (Prevedel et al. 2019; Hepburn et al. 2020). Strain-imaging elastography determines relative differences in stiffness by measuring the displacement fields resulting from some external loading. The loading can

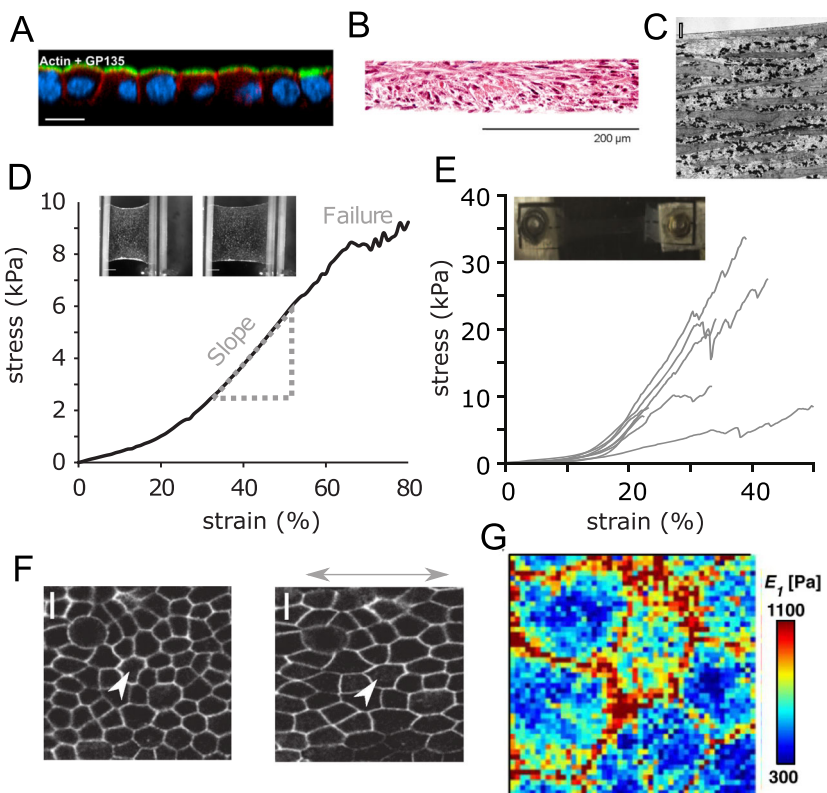


**Fig. 3** Structure and mechanical properties of cell sheets. (A) Confocal cross-section of a suspended MDCK-II cell monolayer, F-actin is shown in red, an apical polarity marker gp135 is shown in green; nuclei are shown in blue. Scale bar is 100  $\mu$ m. Reprinted from (Harris et al. 2012) with permission, copyright 2012 National Academy of Sciences. (B) Detached cell sheet tissue structure of human umbilical cord mesenchymal stem cells with hematoxylin and eosin staining. Reprinted from (Bou-Ghannam et al. 2021), CC BY-4.0, published by Springer Nature. (C) Transmission electron microscopy of a cell sheet of bovine aortic smooth muscle cells showing multiple layers of cells interspersed with considerable ECM (cells are long gray regions, collagen are small, fibrillar elements, elastin are black regions). Scale bar is 2  $\mu$ m. Reprinted from (Isenberg et al. 2012) with permission from Elsevier, copyright 2012. (D) Stress-extension curve of a suspended MDCK-II cell

monolayer. Reprinted from (Harris et al. 2013) with permission from Springer Nature, copyright 2013. Inset: bright-field microscopy images of a monolayer before and during the stretch. Reprinted from (Khalilgharibi et al. 2019) with permission from Springer Nature, copyright 2019. (E) Stress-strain behavior of vascular smooth muscle cell sheets. Inset: sample glued to mounts in the stretching setup. Reprinted from (Backman et al. 2017b) with modifications with permission from Elsevier, copyright 2017. (F) Image of cell boundaries before and after the application of stretch. Scale bar, 10  $\mu$ m. Reprinted from (Harris et al. 2013) with permission from Springer Nature, copyright 2013. (G) Nanomechanical mapping over MDCK cell monolayer with AFM, the color-coded map of viscoelastic modulus. Reprinted from (Efremov et al. 2021) with permission, copyright 2021 The Japan Society of Applied Physics

be applied globally, e.g., by isotropic osmo-mechanical stress caused by the addition of the large non-penetrating molecules to the medium (Leroux et al. 2015), or locally, e.g., by micro-manipulators (Jaiswal et al. 2019) (Fig. 4E). The local displacements in the sample are tracked via different techniques, e.g., differential interference contrast (DIC) or OCT, and then used to calculate the strain distribution via numerical algorithms, such as digital image (volume) correlation (Nahas et al. 2013). The local modulus can be further calculated with additional assumptions and modeling (Leroux et al. 2015).

The method of cavitation rheology was applied to measure the interfacial properties and the elastic modulus of spheroids (Blumlein et al. 2017). A thin needle is inserted into the spheroid under the microscope control, and then the bubble of liquid (cavitation medium) is formed by applying positive pressure. The work of bubble formation is related to the local

mechanical properties, and by varying the needle diameter, these properties can be measured at different length scales (e.g., cellular and intercellular) (Blumlein et al. 2017).

Most of the described tests can be performed in the stress relaxation or creep regimes (Shafiee et al. 2017; Khalilgharibi et al. 2019) or even with dynamical mechanical analysis (DMA) (Gonçalves et al. 2017) to analyze viscoelastic behavior of samples. In addition to the techniques described in this section, other techniques have also been developed to measure stresses and forces in the cell samples, both in 2D (traction force microscopy (TFM), micropillar arrays, monolayer stress microscopy), and 3D conditions (servo-null methods, inclusions, Förster resonance energy transfer (FRET) tension sensors, laser ablation, and force inference). We address the interested reader to a recent review article (Gómez-González et al. 2020) where these techniques are described.

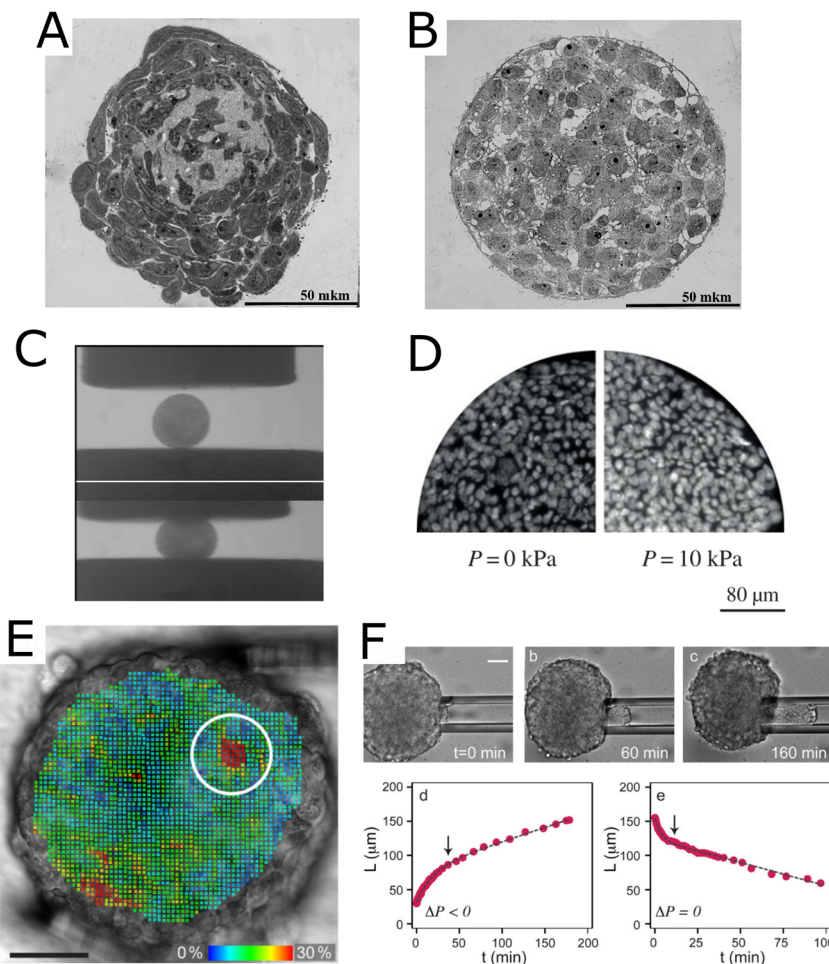


**Fig. 4** Structure and mechanical properties of cell spheroids. (A, B) Semi-fine sections, light microscopy of spheroids made of the limbal MSCs (A) and retinal pigment epithelium cells (B). Scale bars are 50  $\mu\text{m}$ . Reprinted from (Kosheleva et al. 2020), CC BY-4.0, published by Springer Nature. (C) Snapshots of uncompressed (top) and compressed (bottom) embryonic chicken cardiac cushion tissue spheroids, parallel-plate compression setup. Reprinted from (Norotte et al. 2008) with permission from EPL, copyright 2008. (D) Cross-sections of spheroids from HT29 cells with DAPI-stained nuclei for zero (left) and 10 kPa (right) osmotic pressure applied using osmotic effect. Internuclear distances indicate that cell density increases mostly at the center of the spheroid under pressure. Reprinted from (Delarue et al. 2014) with

permission from the Royal Society, copyright 2014. (E) Strain analysis made through 3D pattern tracking during compression with micromanipulators, Von Mises strains are color-coded. Spheroid from a breast tumor cell line BT474, encircled is the position of the soft single-cell-sized spot (Jaiswal et al. 2019). Scale bar is 50  $\mu\text{m}$ . (F) Micropipette aspiration of spheroid made of murine sarcoma cell line S180. Bottom: aspiration and retraction cycles,  $L$  is an advancement of the spheroid inside the pipette, arrows indicate the transitions from elastic to viscous regimes. Scale bar is 50  $\mu\text{m}$ . Reprinted with permission from (Guevorkian et al. 2010), copyright 2010 by the American Physical Society

## Mechanical properties of cell sheets

Despite their seeming simplicity, cell sheets are complex systems where both cell-cell and cell-ECM interaction play substantial roles. Cell sheets can present as a single layer of cells (cell monolayer) almost without ECM (Fig. 3A), but they can also present as well might be composed of multiple layers of cells interspersed with a considerable amount of ECM (Fig. 3B, C). The structure of the cell sheet is determined by the preparation procedure and type (or types) of cells, as described below.

One of the experimental preparation systems produces a suspended epithelial monolayer (Fig. 3D), a one-cell-thick

sheet resembling epithelia in organs, such as acini in the mammary gland or alveoli in the lung (Harris et al. 2013). Suspended epithelial monolayers obtained by enzymatic digestion of temporary collagen substrate have a minimal amount of ECM but maintain polarity and intercellular junctions. Studies performed on such systems have revealed that, similar to the single-cell level, the actomyosin cytoskeleton is a key determinant of mechanical behavior (Harris et al. 2012). Stress relaxation occurs with similar dynamics and in a similar fashion in response to perturbations of the actomyosin cytoskeleton, i.e., softening by actin disruption or contractility inhibition (Harris et al. 2012; Khalilgharibi et al. 2019). Intercellular junctions form stable connections between cells,

maintaining monolayer integrity (Harris et al. 2012). Epithelial monolayers can withstand a doubling in length before failing through rupture of the junctions (Harris et al. 2012). Intermediate filaments progressively stretch during extension, but probably participate in monolayer mechanics at high strains (Harris et al. 2012). During the experimental time scales (several minutes), there are generally no cell rearrangements or divisions, and extension is compensated by monolayer thinning (Harris et al. 2012). The actomyosin-generated pre-tension explains such features as folding and buckling of epithelial monolayer during compression (Wyatt et al. 2020), and curling at the free edges (Fouchard et al. 2020), which are related to epithelial shaping during morphogenesis. The elastic modulus of the epithelial monolayer at extension (20 kPa) was found to be larger than the modulus of single cells (up to several kPa), yet it is considerably low (Harris et al. 2012). The interactions between actomyosin structures of cells via E-cadherin-dependent cell-cell junctions cause a long-range correlation in the mechanical properties of individual cells in the monolayer (Fujii et al. 2019).

Several theoretical models have been developed to describe the mechanics of epithelia (Graner and Glazier 1992; Magno et al. 2015; Alt et al. 2017; Xi et al. 2019). They generally utilize an energy-based approach with several energy components related to internal cell pressure, actomyosin cortex contractility, and intercellular adhesion. The cellular Potts model (CPM) represents the cells as a collection of pixels on a fixed lattice (Graner and Glazier 1992). An energy function is applied to represent different system mechanisms, including energies of individual bonds between lattice sites and the energy cost of individual cells. A minimum energy configuration is then found iteratively. On the other hand, the vertex model (VM) does not require the use of the fixed lattice and represents the cells as vertices and edges, to which energy terms and equations of motion are applied (Alt et al. 2017). Overall, such models can describe well the collective motion and deformation of a large number of cells, and also reproduce some aspects of the experimentally observed epithelial cell monolayer mechanics (Merzouki et al. 2016).

Epithelial monolayers usually have only a small amount of ECM, present in the form of a basement membrane (BM) that lines the basal side of epithelial and endothelial cells. The BM is mainly composed of collagen IV, laminin, the sulphated glycoprotein nidogen, and heparan sulfate proteoglycans (Yurchenco 2011; Khalilgharibi and Mao 2021). Non-fibrillar collagen IV and laminins form two independent but linked networks (Mak and Mei 2017). The BM can have a thickness ranging from less than 100 nm and up to more than 10  $\mu\text{m}$ , and a corresponding stiffness from several kPa, which is close to the stiffness of single cells, up to several MPa (Khalilgharibi and Mao 2021). Therefore, there is a point where ECM mechanics cannot be ignored and at which their involvement starts to dominate the mechanics of the cell sheet.

The ECM might be even more important for other cell types that synthesize fibrillar collagens (types I, II, and others) (Bella and Hulmes 2017). Oriented and aligned collagen fibril deposition can result in extremely stiff tissue structures, such as cartilage and pericardium, where the elastic moduli can reach more than 100 MPa (Grebenik et al. 2019). Further data on ECM mechanics may be derived from the measurement of decellularized tissues, e.g., as for (Jorba et al. 2017), or decellularized ECM produced in cell culture, e.g., as per (Tello et al. 2016).

The ECM is normally produced by cultured cells, and its deposition can be stimulated by prolonged cultivation, the addition of ascorbic acid, and molecular crowding (Kumar et al. 2015). The study of cell sheets with retained ECM generally requires non-enzymatic release from the support (Bou-Ghannam et al. 2021). The actomyosin-generated pre-tension causes contraction, shrinkage, and folding of the monolayer after detachment from the support with reduction of the cross-sectional area by up to 80% (Ando et al. 2008; Bou-Ghannam et al. 2021)), generally with a formation of the multilayered cell sheet (Fig. 3B). It was indeed shown that longer cultivation time, as well as the addition of ascorbic acid to the cell medium, leads to a higher elastic modulus of the cell sheet (Ando et al. 2008). Several weeks of cultivation (up to 10 weeks) were also shown to lead to a high elastic modulus (over 8 MPa) of detached multi-layered cell sheets (Isenberg et al. 2012). Another way to modulate the cell sheet's mechanical properties is the use of micropatterned substrates. The growth of smooth muscle cells on micropatterned substrates consisting of large arrays of alternating grooves and ridges led to a strong alignment of both the cells and ECM in the direction of the micropattern and mechanical anisotropy of the cell sheet (Isenberg et al. 2012). Both the stiffness and strength were significantly higher in the direction of alignment. Such anisotropy is similar to that of native vessels. Moreover, monolayer vascular smooth muscle cell (VSMC) sheets and bilayer VSMC patches displayed nonlinear anisotropic stress-stretch response similar to the biomechanical characteristic of a native arterial wall, with higher modulus at high strains (Backman et al. 2017a; Rim et al. 2018). Cell sheets with high elastic modulus were also obtained from stem cells of different sources (Ando et al. 2008; Roberts et al. 2019), including induced pluripotent stem cells (Kwong et al. 2019) and cells under specific differentiation conditions. Other ways tested to increase mechanical strength involved the addition of collagen type I to the culture medium (resulting in its increased incorporation within the cell sheets and concomitant increase in Young's modulus) (Zhu et al. 2021), the layer-by-layer coating of cell sheets with collagen type I and alginic acid (Yang et al. 2017), magnetic stimulation of the cell sheet with incorporated magnetic nanoparticles (Gonçalves et al. 2017), and the stacking of several cell sheets (Rim et al.

2018). The data on the mechanical properties of cell sheets are summarized in Table 1.

## Mechanical properties of cell spheroids

The mechanical properties of cell spheroids were also found to be determined by an interplay of the cellular actomyosin forces, intercellular interactions, and ECM, as described below. Spheroid formation from dispersed cells consists of three critical steps (Lin and Chang 2008). At the first stage, long-chain ECM fibers are essential for providing loose bonding and aggregation of cells via RGD-integrin interactions. Then, there is a delay stage during which cadherins are expressed and accumulated at the membrane surface. Finally, cells are compacted into solid spherical aggregates due to the cadherin binding and action of actomyosin motors (Fig. 4A, B).

As in the case of cell sheets, general processes that lead to softening of individual cells also lead to the softening of the spheroid as well. The most pronounced effects come from disruption of the actin cytoskeleton (Tsai et al. 2015; Gryadunova et al. 2020), which causes softening and prevents the formation and compactization of the spheroid. The inhibition of the phosphorylation of Rho-associated kinase (ROCK) that reduces actin-myosin contractility has also been shown to prevent spheroid compaction (Tsai et al. 2015). In comparison, disruption of the other two cytoskeletal networks — microtubules and intermediate filaments — had a lesser effect on spheroid stiffness and formation, although disruption of microtubules was shown to somewhat enhance spheroid stiffness (Gryadunova et al. 2020) — a phenomenon also observed in experiments on single cells (Al-Rekabi et al. 2014). Overall, the softer cells seem to produce softer spheroids and vice versa. For example, spheroids from tumor cells are softer than spheroids from their healthy counterparts (Jaiswal et al. 2017), which is also observed on a single-cell level (Lekka et al. 2012). Spheroids from myoblasts and mesenchymal stromal cells were stiffer than spheroids from epithelial cells (Koudan et al. 2020; Kosheleva et al. 2020).

The ECM plays an important role both in promoting spheroid formation and in defining its mechanical properties (Ivascu and Kubbies 2006; Jaiswal et al. 2017). Addition of the basement membrane extract Matrigel to the medium accelerated the formation of compact spheroids from tumor cells (Ivascu and Kubbies 2006). Some specific types of spheroids can be formed only if grown in a matrix rich in basal membrane constituents, namely a lumen-like hollow center spheroids where cells of the outermost layer form a polarized epithelium with the apical surface pointing inward (Weaver et al. 2002; Lee et al. 2007). The elastic modulus of spheroids from chondrocytes was shown to substantially increase with cultivation time (more than a 5X increase from day 1 to day 21) with this increase associated with the synthesis and accumulation of the ECM components, type II collagen, and aggrecan (Omelyanenko et al.

2020). AFM indentational mapping of spheroids revealed that the presence of the stiffer regions most likely originated due to the collagen-based fibrillar structures (Vyas et al. 2019). Treatment of tumor spheroids with collagenase led to a decrease in the elastic modulus by half (Jaiswal et al. 2017), and also to an increase in nanoparticle penetration caused by the weakening of the ECM and spheroid integrity (Goodman et al. 2007).

The mechanical properties of spheroids were found to be non-homogenous. When osmo-mechanical stress was applied to the spheroids by adding dextran to the culture medium, it led to an overall decrease of the spheroid's volume. However, the compression was higher for the cells in the spheroid core, which indicates that the inner cell mass is softer than the external layer (Leroux et al. 2015) (Fig. 4D). Yet, it might also be explained by an anisotropic arrangement of cells combined with the active tension of cells in response to pressure (Dolega et al. 2017). The theory suggested by Delarue et al. (Delarue et al. 2014) also takes into account the dependence of cell division and apoptosis rates on the local stress, the cell polarity and active stress generated by the cells, and the dependence of active stress on the local pressure. In line with theory, it was demonstrated that external stress can inhibit cell proliferation in the core of a spheroid made of cancer cells (Montel et al. 2011, 2012). The presence of the stiff envelope and the soft core was also revealed in parallel-plate compression experiments with mathematical analysis of spheroid shape relaxation (Yu et al. 2018). However, further experiments are needed to discriminate between active cell responses, differences in different cell layers mechanical properties, contractility, and tension at different experimental times.

Although spheroids are often considered as elastic or viscoelastic solids, their description as a liquid with surface tension is very effective, especially to describe longer time processes like spheroid formation and fusion (Steinberg 1963; Foy et al. 1994; Gonzalez-Rodriguez et al. 2012; Shafiee et al. 2019a). Spheroid formation, as well as cell sorting and spheroid fusion processes, is in a way similar to the behavior of liquid, a medium consisting of molecules, whose behavior is governed by attractive forces at the molecular scale yielding continuum properties of viscosity and surface tension at the macroscale. The principle of surface tension is used to explain the tendency of a liquid to minimize its total surface, and thus, the apparent tissue surface tension (ATST) can be used by analogy to describe spheroid formation (Norotte et al. 2008). Effects of the surface tension can be directly observed in experiments where the opening of spheroids occurs after an incision (an increase of distance between the two sides of the cut) (Czajka et al. 2014; Kosheleva et al. 2016; Guillaume et al. 2019). The fusion of two or more spheroids can be described based on the ATST as well (Shafiee et al. 2019b, a).

Predictions of the ATST concept, also known as tissue liquidity, have been confirmed in many *in vitro* experiments. Both intercellular adhesions and actomyosin-mediated tension contribute to ATST, and several theories have been developed

**Table 1** Mechanical properties of cell sheets

Parameters of the cell sheet	Measurement details	Elastic modulus/stiffness	Failure stress/ ultimate tensile strength	Failure strain	Reference
Human MSCs from synovial membranes grown on cell culture plastic for 3–21 days (four time points), detachment by gentle pipetting	Custom-made uniaxial tensile tester	~3.51 MPa (+AA, 14 day) ~5.23 MPa (+AA, 21 day) 0.11 MPa (-AA, 14 day) ~0.28 MPa (-AA, 21 day)	~0.76 MPa (+AA, 14 day) 1.32 ± 0.25 MPa (+AA, 21 day) ~0.01 MPa (-AA, 14 days) ~0.10 MPa (-AA, 21 day)	—	(Ando et al. 2008)
Suspended monolayers of MDCK cells, treatments with Latrunculin B (depolymerization of actin cytoskeleton), Y27632 (inhibitor of contractility), and EDTA (block of cadherin-mediated adhesion)	Stretching of monolayer suspended between the test rods with a micromanipulator	Control: 20 ± 2 kPa Latrunculin B: 10 ± 6 kPa Y27632: 13 ± 6 kPa EDTA: 0.8 ± 0.4 kPa	—	Control: ~0.7 Latrunculin B: ~0.7 Y27632: ~0.7 EDTA: ~0.2	(Harris et al. 2012, 2013)
Monolayer of human pulmonary epithelial cells A549 on PDMS membrane	Equibiaxial stretching of the PDMS membrane with adherent cells	40 ± 8 kPa	—	—	(Dassow et al. 2013)
Bovine aortic SMCs, grown on patterned (p) and non-patterned (n/p) substrates, spontaneous detachment after 10 weeks of cultivation	Custom-built uniaxial tensile tester	Stiffness: 7.35 ± 1.68 MPa (n/p) 8.95 ± 2.05 MPa (p, parallel)	3.41 ± 0.72 MPa (n/p) 3.89 ± 1.26 MPa (p, parallel)	0.53 ± 0.074 (n/p) 0.50 ± 0.10 (p, parallel)	(Isenberg et al. 2012)
Bovine aortic SMCs grown for 11 days on PNIPAAm–PDMS substrates	Custom uniaxial tensile tester, Hall-Effect based force sensor	Young's modulus: 114.2 ± 33.5 kPa	155.2 ± 98.2 kPa	0.32 ± 0.10	(Backman et al. 2017b)
Bovine aortic SMCs grown for 17–21 days on patterned (p) and non-patterned (n/p) PNIPAAm–PDMS substrates	Custom uniaxial tensile tester, Hall-Effect based force sensor	932 ± 102 kPa (n/p) 2995 ± 961 kPa (p, parallel)	225 ± 28.5 kPa (n/p) 410 ± 140 kPa (p, parallel)	0.75 ± 0.05 (n/p) 0.43 ± 0.1 (p, parallel)	(Backman et al. 2017a)
Bovine aortic SMCs grown on patterned (p) and non-patterned (n/p) tyramine-conjugated carboxymethyl cellulose or alginate hydrogel for 10–14 days, stacked cell sheets	Custom uniaxial tensile tester, Hall-Effect based force sensor	253.62 ± 39.86 kPa (n/p) 376.81 ± 21.74 kPa (p, parallel)	187.23 ± 44.68 kPa (n/p) 221.28 ± 10.64 kPa (p, parallel)	3.53 ± 0.21 (n/p) 2.32 ± 0.14 (p, parallel)	(Rim et al. 2018)
Placental mesenchymal stem cells (with cardiac differentiation) grown on tyramine-conjugated alginate hydrogel for 10 days	Custom uniaxial tensile tester, Hall-Effect based force sensor	22.0 ± 5.74 kPa	12.4 ± 7.51 kPa	0.78 ± 0.16	(Roberts et al. 2019)
Murine and human iPSCs (with SMCs differentiation), immortalized mouse aortic vascular SMCs (as a control) grown on tyramine-conjugated alginate hydrogel for 4–6 weeks	Custom uniaxial tensile tester, Hall-Effect based force sensor	Elastic modulus: 235.1 ± 147.4 kPa (murine) 49.1 ± 31.6 kPa (human) 154.4 ± 63.2 kPa (control)	94.57 ± 60.87 kPa (murine) 32.61 ± 14.13 kPa (human) 20.65 ± 8.70 kPa (control)	0.72 ± 0.34 (murine) 0.81 ± 0.18 (human) 0.71 ± 0.30 (control)	(Kwong et al. 2019)

**Table 1** (continued)

Parameters of the cell sheet	Measurement details	Elastic modulus/stiffness	Failure stress/ ultimate tensile strength	Failure strain	Reference
C2C12 and NIH-3T3 cells grown on thermoresponsive surface (PNIPAAm) for 5 days, treated or not treated with cytochalasin D	Custom-made uniaxial tensile tester	27.1 kPa (3T3) and 20.1 kPa (C2C12) for untreated cell sheets 2.2 kPa (3T3) and 7.5 kPa (C2C12) for treated cell sheets	27–53 $\mu$ N (untreated cell sheets) 16–91 $\mu$ N (treated cell sheets)	0.03–0.2 (untreated cell sheets)	(Uesugi et al. 2013)
Human ASCs, tenomodulin positive subpopulation grown on cell culture plastic in a presence of iron oxide nanoparticles, detachment with a magnet for 7 days	Dynamic mechanical analysis equipment (tensile mode)	$36.34 \pm 5.60$ MPa at 2 Hz	—	—	(Gonçalves et al. 2017)
Monolayers of MDCK II and sarcoma osteogenic cells SaOS2	Stretching of monolayers growing on a soft suspended membrane	$23.3 \pm 6.3$ kPa for MDCK $72.9 \pm 10.3$ kPa for SaOS2	—	—	(Sorba et al. 2019)
Bone marrow stromal cells grown on PDMS for 2 weeks, mechanical detachment, constructs made of aligned (a) or non-aligned (n/a) cell sheets	Compression and flexural tests on commercial devices	Compressive modulus: $319.00 \pm 112.09$ kPa (a) flexural modulus: $31.84 \pm 10.12$ kPa (a) $14.42 \pm 10.12$ kPa (n/a)	—	—	(Chuah et al. 2020)

to describe this contribution. The Differential Adhesion Hypothesis (DAH), proposed by Steinberg (Steinberg 1963), suggests that tissue surface tension is determined by the level of expression of cell adhesion molecules, which modulate the strength of the adhesive energy between the constituent cells (treated as point objects in the model). Some predictions of DAH theory were confirmed in *in vitro* experiments with cells expressing different levels of N-, P-, or E-cadherins showing that surface tension is a function of cadherin expression level (Foty and Steinberg 2005). The Differential Surface Contraction Hypothesis (DSCH) proposes that surface tension arises primarily from differences in actomyosin-driven cell cortical contractility (Harris 1976). Finally, the Differential Interfacial Tension Hypothesis (DITH) states that differences in interfacial tensions depend both on intercellular adhesion and cell contractility with some competing effects, thus combining ideas of the DAH and the DSCH (Brodland 2002; Manning et al. 2010).

Spheroids from different types of cells are expected to have different ATST. *In vivo*, organs, tissues, and cells can respond to external disturbances by maintaining a certain homeostatic level of tension, giving rise to the concept of tensional homeostasis (Stamenović and Smith 2020). At the level of isolated cells and small clusters, the tensional homeostasis was found to be cell type-dependent and also greatly affected by the cell-cell contacts and cell-cell adhesion molecules (Zollinger et al. 2018). Related to the tensional homeostasis phenomena are mechanosensing and mechanotransduction, an ability of a cell to sense mechanical signals from its environment and translate them into a cellular response, respectively (Jansen et al. 2015). From this point of view, spheroids represent an isolated object, where the balance of such processes leads to the homeostatic ATST level, which should be related to the tissue origin of the spheroid-forming cells. The homeostatic ATST achieved in 3D spheroid can translate into biological effects, such as increased levels of tissue-specific markers and the gaining of tissue-specific functions. Some mechanical effects have also been observed, such as an increase of surface tension with the applied force and pulsed contractions (or “shivering”), which are interpreted as effects of cellular mechanosensing (Guevorkian et al. 2010, 2011). The data on the mechanical properties of cell spheroids are summarized in Table 2.

## Relationship between the mechanical properties of single cells, extracellular matrix, and tissues

Currently, there is a significant amount of data on mechanics at the single cells and tissue levels, but equivalent information about intermediate multicellular structures is conspicuously less. Single cells are known to possess viscoelastic behavior

that is principally governed by the actomyosin cytoskeleton, mainly presented in the sub-membrane layer (actin cortex) and in the form of stress fibers, which are manifest by long contractile actin bundles linked either to the cell-ECM contacts (focal adhesions) or cell-cell contacts (adherens junctions) (Chugh and Paluch 2018; Efremov et al. 2019b; Jung et al. 2020). The actin cortex regulates cell surface tension, and stress fibers are generally associated with both high cell stiffness and high traction forces applied by cells to the substrate. The apparent bulk elastic modulus, which might be prescribed to cells based on different measurement techniques, is rather low, in the range of 0.1–10.0 kPa (Wang et al. 2018; Wu et al. 2018). Data on cell sheets and spheroids indicate that stiffer cells also produce stiffer multicellular structures. Moreover, the bulk mechanical properties of the cell sheet/spheroid might be close to that of the single cell, at least before an accumulated ECM starts playing a major role (Isenberg et al. 2012; Omelyanenko et al. 2020). However, there also might be a difference in properties between cells growing on stiff 2D substrates and cells in spheroids. For example, some cells become stiffer when grown on stiff cell culture-plate p plastic (Solon et al. 2007; Janmey et al. 2020), while in spheroids, where the mechanical surrounding is provided by the neighbor cells, a soft microenvironment is created. Thus, cells recover the soft phenotype, which is close to the native conditions.

The situation changes, however, when ECM is accumulated within the cell aggregate. The ECM fibers possess elastic modulus at extension in a range from several MPa (elastin) to several GPa (collagen) (Aaron and Gosline 1981; Wenger et al. 2007; Guthold et al. 2007; Guimarães et al. 2020). However, the mechanical properties of the matrix consisting of ECM fibers will significantly vary based on the structural differences, fiber orientation and linkage, and interaction of different fiber types (Black et al. 2008; Akhmanova et al. 2015; Padhi and Nain 2020). *In vivo*, cross-linking and other post-translational enzymatic ECM modifications will have a strong impact on its properties. High stiffness of non-mineralized tissues (several MPa) might be achieved by proper structuring of the ECM, as in some connective tissues (e.g., skin, cartilages, tendons, ligaments, fibrous pericardium). The cellular component plays a minor mechanical role in such tissues since its removal (decellularization) weakly affects the mechanical strength of the isolated tissue (Melo et al. 2014; Nonaka et al. 2014). Nevertheless, the regulatory role of cells remains critical since they maintain the ECM by producing, remodeling, and degrading it. Dysregulation of these processes will eventually lead to changes in bulk mechanical properties of the ECM, observed as different pathologies (Sonbol 2018).

There have been a number of attempts to synthetically recreate the ECM, by such procedures as fiber pulling, wet spinning, electrospinning, collagen crowding, and confinement (Hoffmann et al. 2019). However, most such methods of

**Table 2** Mechanical properties of spheroids

Parameters of spheroid	Measurement details	Mechanical parameter	Reference
Spheroids of chick embryonic heart ventricle and liver cells	Parallel plate compression	Surface tension: $4.3 \pm 0.1$ mN/m (liver) $8.3 \pm 0.1$ mN/m (heart)	(Foty et al. 1994)
Spheroids of CHO cells, human umbilical smooth muscle cells (HUSMC), human umbilical vein endothelial cells (HUVEC)	Parallel plate compression	Apparent tissue surface tension: $22.8 \pm 3.0$ mN/m (CHO) $12.0 \pm 0.2$ mN/m (HUVEC) $279 \pm 57$ mN/m (HUSMC)	(Norotte et al. 2008)
Spheroids of chick embryonic tissues	Parallel plate compression	Cell-medium surface tension: $12.9 \pm 0.9$ N/m (mesencephalon) $14.1 \pm 2.2$ N/m (neural retina) $23.3 \pm 2.4$ N/m (liver) $72.4 \pm 11.0$ N/m (heart) Cytoplasm viscosity: $27.1 \pm 3.0$ Pa·s (mesencephalon) $20.4 \pm 3.4$ Pa·s (neural retina) $39.5 \pm 3.3$ Pa·s (liver) $60.7 \pm 7.2$ Pa·s (heart)	(Brodland et al. 2009)
Spheroids of murine sarcoma (S180) cell lines transfected to express various levels of E-cadherin molecules	Micropipette aspiration	Surface tension at rest: $\sim 0.6$ mN/m viscosity: $1.9 \pm 0.3 \times 10^5$ Pa·s elastic modulus: $700 \pm 100$ Pa	(Guevorkian et al. 2010)
Spheroids of human colon adenocarcinoma cancer cell line LS174T	AFM, different cantilever velocities	Apparent elastic modulus: $311 \pm 9$ Pa at $2.5 \mu\text{m}/\text{s}$ $488 \pm 48$ Pa at $10.0 \mu\text{m}/\text{s}$ $539 \pm 27$ Pa at $20.0 \mu\text{m}/\text{s}$	(Mills et al. 2011)
Spheroids of human bone marrow-derived mesenchymal stem cells (hMSCs) with incorporated gelatin microparticles	Parallel-plate compression	Young's modulus: $62.40 \pm 5.58$ Pa (control) $240.98 \pm 23.19$ Pa (with incorporated gelatin microparticles)	(Baraniak et al. 2012)
Spheroids of HT29 (human colon carcinoma) and BC52 (human breast cancer) cell lines	Osmo-mechanical stress	compressional modulus: $40 \pm 20$ kPa (HT29) $16 \pm 5$ kPa (BC52)	(Delarue et al. 2014)
Spheroids of HEK 293 cells	Cavitation rheology using different needle diameters (D)	Local elastic modulus: $\sim 32$ Pa ( $D = 30 \mu\text{m}$ ) $\sim 67$ Pa ( $D = 10 \mu\text{m}$ ) $\sim 220$ Pa ( $D = 5 \mu\text{m}$ )	(Blumlein et al. 2017)
Spheroids of NIH 3T3 fibroblasts	Colloidal probe AFM	Young's modulus in the range of $0.5\text{--}3.5$ kPa	(Jorgenson et al. 2017)
Spheroids of two cancerous (T47D and BT474) and one normal epithelial (MCF 10A) breast cell lines	Microtweezers	Young's moduli: $230$ Pa (BT474) $420$ Pa (T47D) $1250$ Pa (MCF 10A)	(Jaiswal et al. 2017)
Spheroids of primary sheep chondrocytes	Parallel-plate compression	Secant modulus of elasticity: $2.2 \pm 0.2$ kPa (1 day-old) $4.6 \pm 0.2$ kPa (7 days-old) $8.5 \pm 0.8$ kPa (14 days-old) $17.5 \pm 1.2$ kPa (21 days-old)	(Omelyanenko et al. 2020)
Spheroids of human mesenchymal stem cells (MSC) from the limbal eye stroma and epithelial cells from retinal pigment epithelium (RPE)	Nanoindenter	Young's modulus: $3.94 \pm 0.81$ kPa (MSC) $1.63 \pm 0.34$ kPa (RPE)	(Kosheleva et al. 2020)
Spheroids of HEK293, primary human fibroblasts (HF), primary sheep chondrocytes, and rat myoblast cell line L6	Parallel-plate compression	Secant modulus of elasticity (along with maturation time): $0.2$ to $0.4$ kPa (HEK293) $0.7$ to $5.4$ kPa (L6) $0.8$ to $4.7$ kPa (chondrocytes) $1.5$ to $3.3$ kPa (HF)	(Koudan et al. 2020)

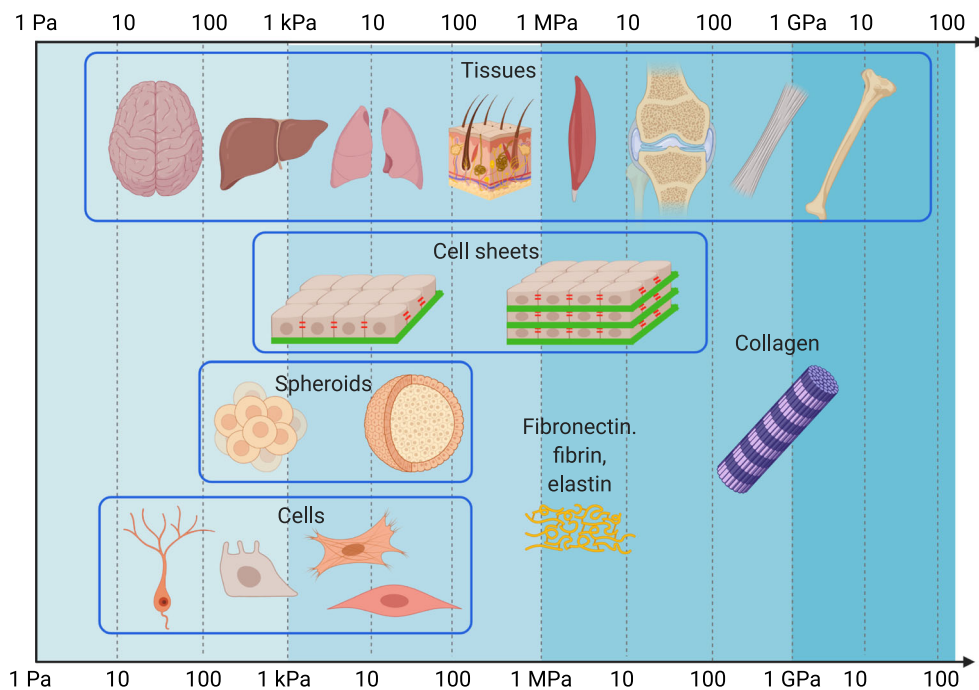


**Fig. 5** The stiffness of cell sheets and spheroids relative to the stiffness of single cells, tissues, and some ECM molecules. The elastic moduli ( $E$ ) are reported on the logarithmic scale. The cells generally have stiffness in the range from the tens of Pa (mucus, neural tissues) to the several hundreds of kPa, with the neurons among the softest cells and the muscle cells among the stiffer cells. The tissues span a larger range from the tens of Pa to the several GPa (Guimarães et al. 2020). Depicted from the softest to

the stiffest: neural tissues, liver, lung, skin, muscle tissues, cartilage, tendon, and bone. Reported values of spheroid stiffness are close to such of single cells. Cell sheets show an elastic modulus close to cells with higher values up to the several MPa, generally associated with the multilayered structure and higher ECM content. The values of the ECM molecules (fibronectin, fibrin, elastin, collagen) are included for comparison

synthetic generation of ECM fibers and matrices currently use only a single type of ECM protein and lack posttranslational modifications. The compositional and structural complexity of native ECM has not been recreated. Moreover, the achievement of a proper understanding of the mechanical properties of the native fibrillar connective tissues has as yet not been achieved. In general, *in vitro* attempts to replicate their mechanical properties require additional means for increasing the construct stiffness. Among such are chemical cross-linking and incorporation of stiff synthetic polymers (Kaiser and Coulombe 2015; Delgado et al. 2015). Synthetic ECM constructs also cause difficulties with cell seeding and distribution through the entire volume. On the other hand, cell sheets with a high amount of ECM might resolve the mentioned problems, and indeed a balance between cell distribution and stiffness in such cell sheets has been observed (Ando et al. 2008; Isenberg et al. 2012). Complex microtissues, containing both cells and cell-generated ECM, can be created by stacking cell sheets or fusing cell spheroids (Norotte et al. 2009; Rim et al. 2018).

The quantity of ECM present in tissues, in particular type I collagen, was shown to be proportional to tissue microelasticity (Swift et al. 2013). Overall, the elastic moduli of human tissues (as measured by macroscale techniques) span a huge range from the tens of Pa (mucus, neural tissues)

to the several GPa (bones) (Guimarães et al. 2020) (Fig. 5). The proper and simultaneous accounting of the mechanical properties of both cellular and ECM components in a complex biological system is a difficult task for analysis and modeling, especially *in vivo*. For example, there is an intricate balance between cells and ECM in lung alveoli (Roan and Waters 2011; Knudsen and Ochs 2018; Yang et al. 2020). The mechanical stability is provided by several components: connective tissue fiber network, continuous alveolar epithelium and capillary endothelium, and surfactant system, produced by epithelial cells (Knudsen and Ochs 2018). Lung ECM has a stiffness of tens of kPa that is not much higher than that of its component cells (Jorba et al. 2017). However, it is unclear if the cellular components contribute substantially to overall lung mechanical properties since there are only minor changes after decellularization of the lung tissue (Nonaka et al. 2014). Surfactant, the surface film of lipids and proteins at the air-liquid interface, is essential for lung function since it prevents alveolar collapse by reducing alveolar surface tension. Despite considerable efforts over the last decades, a comprehensive understanding of alveolar micromechanics is still missing, mostly due to the impossibility of direct measurement of alveolar stress and strain *in vivo*. Therefore, a simpler model system might shed light on some micromechanical processes related to

mechanical interactions of cellular and ECM components under different conditions.

Even at the level of cellular aggregates such as cell sheets and spheroids, the effect of ECM in contributing to mechanical balance is not fully resolved. It should be noted that there are well-developed models that concentrate on intercellular interactions, such as Cellular Potts Models and Vertex Models for cell monolayers, DAH, and DITH models for cell spheroids, which are described above. Yet, in those theories, the ECM is not considered as an active component. However, as described above, the ECM affects the global mechanics of cellular aggregates, and might also affect different aspects of cellular behavior. For example, the presence of ECM in spheroids from mesenchymal stromal cells might be an important factor during the spheroid fusion and furthermore might lead to outcomes that are not predicted by cellular-based models (Kosheleva et al. 2020). Recent studies also suggest that the ECM can play the role of a sensor that mechanically regulates cell proliferation and migration in cell spheroids (Dolega et al. 2021a, b). In the experiments, draining the water out of the ECM via the addition of big non-penetrating osmolytes imposed a residual compressive mechanical stress on the cells over a long timescale, and caused a decrease in both cell proliferation and motility in spheroids (Dolega et al. 2021b).

Interactions between ECM and cells are expected to play an even more significant role at the level of microtissues and organoids. Microtissue can be broadly defined as an engineered three-dimensional (3D) structure formed by the functional aggregation of one or more cell types, assembled with or without the support of a scaffold (scaffold-based and scaffold-free microtissues) (Blakely et al. 2013; Patino-Guerrero et al. 2020). Microtissues can be formed by stacking cell sheets or by spheroid fusion. Organoids are generally formed from pluripotent or adult stem cells with self-organization following the principles of the original organ and recapitulation of at least some functions of the organ (Clevers 2016). Mechanobiology of both microtissues and organoids remains poorly studied, although mechanical properties and biomechanical cues were shown to be important during the formation and maintenance of such structures (Bayir et al. 2019; Wechsler et al. 2020).

## Conclusions and future perspectives

The development of cell-sheet and spheroid tissue engineering methods has generated a need for a systematic characterization of cell-cell and cell-ECM interactions in such structures so as to better mimic and condition them for *in vivo* applications. Several challenges need to be overcome for better mechanical characterization of cellular aggregates. While there have been substantial achievements in the characterization of

epithelial monolayers, more complicated structures like multi-layered ECM-containing cell sheets, microtissues, and organoids present a great challenge for both microscopy-based characterization and mechanical modeling. There is a need to improve methods that will allow local volumetric mechanical measurement and observation of distributions of stress and strains in a living aggregate in real time with a good spatial resolution. Elastography techniques, including ones based on OCT and light microscopy, might be a promising tool to reveal the internal properties of the cell aggregates with an improvement of penetration depth.

Relatively simple multicellular structures are good materials for the development and testing of biomechanical models. While there are many models that elaborate on cell-cell interactions, the inclusion of cell-ECM mechanical interaction is a further necessary step that must be achieved. In this regard, modulation of ECM structure can be a dominant way to control the overall mechanical properties of the scaffold-free tissue engineering constructs and the local mechanical environment of the cells.

Currently, the rich mechanical behavior of multicellular structures leads to different ways of describing the same observables, giving rise to concurring theories. For example, resistance to compression of cell spheroids might be considered as a viscoelastic behavior of the solid body, or as the surface tension of the liquid drop; the opening of a spheroid after the incision might be seen as a result of the surface tension or the presence of residual stresses. The time scale of the experiment plays a huge role in aggregate response and data interpretation. At short time scales, which are faster than cellular movements, most of the components of the system will behave as solids in an elastic or viscoelastic way. At longer time scales, when there is a time for the cell movements and even for ECM remodeling, the response might be plastic- or liquid-like. Proper accounting for the time-dependent behavior and establishment of transition times of these complex systems is another important step in modeling.

Overall, multicellular systems like cell sheets and spheroids are promising candidates for studying the effects of intercellular and cell-ECM interactions, as well as the effects of external and internal mechanical forces. Such systems allow us to isolate and modulate certain biochemical and biophysical cues and study their effects on tissue or disease development and regeneration. From the practical perspective, creating proper biophysical cues and mechanical niches for cell activity will improve the quality of the tissue engineering constructs. In the future, acquisition of tissue engineering constructs with the desired macroscale mechanical properties for better handling and toughness during implantation will also undoubtedly be achieved.

**Acknowledgements** Figures 1 and 5 were created with BioRender.com.

**Conflict of interest** The authors declare no competing interests.

**Funding** This work was financed by the Ministry of Science and Higher Education of the Russian Federation within the framework of state support for the creation and development of World-Class Research Centers “Digital biodesign and personalized healthcare” No 075-15-2020-926.

## References

- Aaron BB, Gosline JM (1981) Elastin as a random-network elastomer: a mechanical and optical analysis of single elastin fibers. *Biopolymers* 20:1247–1260. <https://doi.org/10.1002/bip.1981.360200611>
- Akhmanova M, Osidak E, Domogatsky S et al (2015) Physical, spatial, and molecular aspects of extracellular matrix of in vivo niches and artificial scaffolds relevant to stem cells research. *Stem Cells Int* 2015. <https://doi.org/10.1155/2015/167025>
- Akiyama Y, Kikuchi A, Yamato M, Okano T (2004) Ultrathin poly( N -isopropylacrylamide) grafted layer on polystyrene surfaces for cell adhesion/detachment control. *Langmuir* 20:5506–5511. <https://doi.org/10.1021/la036139f>
- Al-Rekabi Z, Haase K, Pelling AE (2014) Microtubules mediate changes in membrane cortical elasticity during contractile activation. *Exp Cell Res* 322:21–29. <https://doi.org/10.1016/j.yexcr.2013.12.027>
- Alt S, Ganguly P, Salbreux G (2017) Vertex models: from cell mechanics to tissue morphogenesis. *Philos Trans R Soc B Biol Sci* 372: 20150520
- Ando W, Tateishi K, Katakai D et al (2008) In vitro generation of a scaffold-free tissue-engineered construct (TEC) derived from human synovial mesenchymal stem cells: biological and mechanical properties and further chondrogenic potential. *Tissue Eng Part A* 14: 2041–2049. <https://doi.org/10.1089/ten.tea.2008.0015>
- Andolfi L, Greco SLM, Tierno D et al (2019) Planar AFM macro-probes to study the biomechanical properties of large cells and 3D cell spheroids. *Acta Biomater* 94:505–513. <https://doi.org/10.1016/j.actbio.2019.05.072>
- Arroyave GAI, Lima RG, Martins PALS et al (2015) Methodology for mechanical characterization of soft biological tissues: arteries. *Procedia Eng* 110:74–81. <https://doi.org/10.1016/j.proeng.2015.07.012>
- Backman DE, LeSavage BL, Shah SB, Wong JY (2017a) A robust method to generate mechanically anisotropic vascular smooth muscle cell sheets for vascular tissue engineering. *Macromol Biosci* 17: 1600434. <https://doi.org/10.1002/mabi.201600434>
- Backman DE, LeSavage BL, Wong JY (2017b) Versatile and inexpensive Hall-Effect force sensor for mechanical characterization of soft biological materials. *J Biomech* 51:118–122. <https://doi.org/10.1016/j.jbiomech.2016.11.065>
- Bakirci E, Toprakhisar B, Zeybek MC et al (2017) Cell sheet based bioink for 3D bioprinting applications. *Biofabrication* 9:024105. <https://doi.org/10.1088/1758-5090/aa764f>
- Baptista L, Kronemberger G, Córtes I et al (2018) Adult stem cells spheroids to optimize cell colonization in scaffolds for cartilage and bone tissue engineering. *Int J Mol Sci* 19:1285. <https://doi.org/10.3390/ijms19051285>
- Baraniak PR, Cooke MT, Saeed R et al (2012) Stiffening of human mesenchymal stem cell spheroid microenvironments induced by incorporation of gelatin microparticles. *J Mech Behav Biomed Mater* 11:63–71. <https://doi.org/10.1016/j.jmbbm.2012.02.018>
- Basoli F, Giannitelli SM, Gori M et al (2018) Biomechanical characterization at the cell scale: present and prospects. *Front Physiol* 9:1–21. <https://doi.org/10.3389/fphys.2018.01449>
- Bayir E, Sendemir A, Missirlis YF (2019) Mechanobiology of cells and cell systems, such as organoids. *Biophys Rev* 11:721–728. <https://doi.org/10.1007/s12551-019-00590-7>
- Bella J, Hulmes DJS (2017) Fibrillar Collagens. In: Parry D, Squire J (eds) Fibrous proteins: structures and mechanisms. Subcellular Biochemistry, 82. Springer, Cham 457–490
- Bhat ZF, Fayaz H (2011) Prospectus of cultured meat—advancing meat alternatives. *J Food Sci Technol* 48:125–140. <https://doi.org/10.1007/s13197-010-0198-7>
- Bhat ZF, Kumar S, Fayaz H (2015) In vitro meat production: challenges and benefits over conventional meat production. *J Integr Agric* 14: 241–248. [https://doi.org/10.1016/S2095-3119\(14\)60887-X](https://doi.org/10.1016/S2095-3119(14)60887-X)
- Bialekowska K, Komorowski P, Bryszewska M, Miłowska K (2020) Spheroids as a type of three-dimensional cell cultures—examples of methods of preparation and the most important application. *Int J Mol Sci* 21:1–17. <https://doi.org/10.3390/ijms21176225>
- Binnig G, Quate CF, Gerber C (1986) Atomic force microscope. *Phys Rev Lett* 56:930–933. <https://doi.org/10.1103/PhysRevLett.56.930>
- Black LD, Allen PG, Morris SM et al (2008) Mechanical and failure properties of extracellular matrix sheets as a function of structural protein composition. *Biophys J* 94:1916–1929. <https://doi.org/10.1529.biophysj.107.107144>
- Blakely AM, Schell JY, Rago AP, et al (2013) Formation of multicellular microtissues and applications in biofabrication. In: Biofabrication: Micro- and Nano-fabrication, Printing, Patterning and Assemblies. Elsevier 149–166
- Blumlein A, Williams N, McManus JJ (2017) The mechanical properties of individual cell spheroids. *Sci Rep* 7:1–10. <https://doi.org/10.1038/s41598-017-07813-5>
- Bou-Ghannam S, Kim K, Grainger DW, Okano T (2021) 3D cell sheet structure augments mesenchymal stem cell cytokine production. *Sci Rep* 11:8170. <https://doi.org/10.1038/s41598-021-87571-7>
- Brodland GW (2002) The Differential Interfacial Tension Hypothesis (DITH): a comprehensive theory for the self-rearrangement of embryonic cells and tissues. *J Biomech Eng* 124:188–197. <https://doi.org/10.1115/1.1449491>
- Brodland GW, Yang J, Sweny J (2009) Cellular interfacial and surface tensions determined from aggregate compression tests using a finite element model. *HFSP J* 3:273–281. <https://doi.org/10.2976/1.3175812>
- Burdis R, Kelly DJ (2021) Biofabrication and bioprinting using cellular aggregates, microtissues and organoids for the engineering of musculoskeletal tissues. *Acta Biomater* 126:1–14. <https://doi.org/10.1016/j.actbio.2021.03.016>
- Chao C, Ngo LP, Engelward BP (2020) SpheroidChip: patterned agarose microwell compartments harboring HepG2 spheroids are compatible with genotoxicity testing. *ACS Biomater Sci Eng* 6:2427–2439. <https://doi.org/10.1021/acsbiomaterials.9b01951>
- Chuah YJ, Tan JR, Wu Y et al (2020) Scaffold-free tissue engineering with aligned bone marrow stromal cell sheets to recapitulate the microstructural and biochemical composition of annulus fibrosus. *Acta Biomater* 107:129–137. <https://doi.org/10.1016/j.actbio.2020.02.031>
- Chugh P, Paluch EK (2018) The actin cortex at a glance. *J Cell Sci* 131: jcs186254. <https://doi.org/10.1242/jcs.186254>
- Clevers H (2016) Modeling development and disease with organoids. *Cell* 165:1586–1597. <https://doi.org/10.1016/j.cell.2016.05.082>
- Conrad C, Gray KM, Stroka KM et al (2019) Mechanical characterization of 3D ovarian cancer nodules using brillouin confocal microscopy. *Cell Mol Bioeng* 12:215–226. <https://doi.org/10.1007/s12195-019-00570-7>
- Cui X, Hartanto Y, Zhang H (2017) Advances in multicellular spheroids formation. *J R Soc Interface* 14:20160877
- Czajka CA, Mehesz AN, Trusk TC et al (2014) Scaffold-free tissue engineering: organization of the tissue cytoskeleton and its effects on

- tissue shape. *Ann Biomed Eng* 42:1049–1061. <https://doi.org/10.1007/s10439-014-0986-8>
- Daly AC, Davidson MD, Burdick JA (2021) 3D bioprinting of high cell-density heterogeneous tissue models through spheroid fusion within self-healing hydrogels. *Nat Commun* 12:753. <https://doi.org/10.1038/s41467-021-21029-2>
- Dassow C, Armbruster C, Friedrich C et al (2013) A method to measure mechanical properties of pulmonary epithelial cell layers. *J Biomed Mater Res - Part B Appl Biomater* 101:1164–1171. <https://doi.org/10.1002/jbm.b.32926>
- Delarue M, Joanny JF, Jülicher F, Prost J (2014) Stress distributions and cell flows in a growing cell aggregate. *Interface Focus* 4:20140033. <https://doi.org/10.1098/rsfs.2014.0033>
- Delgado LM, Bayon Y, Pandit A, Zeugolis DI (2015) To cross-link or not to cross-link? Cross-linking associated foreign body response of collagen-based devices. *Tissue Eng Part B Rev* 21:298–313. <https://doi.org/10.1089/ten.teb.2014.0290>
- Dolega ME, Delarue M, Ingremeau F et al (2017) Cell-like pressure sensors reveal increase of mechanical stress towards the core of multicellular spheroids under compression. *Nat Commun* 8:14056. <https://doi.org/10.1038/ncomms14056>
- Dolega M, Zurlo G, Le Goff M et al (2021a) Mechanical behavior of multi-cellular spheroids under osmotic compression. *J Mech Phys Solids* 147:104205. <https://doi.org/10.1016/j.jmps.2020.104205>
- Dolega ME, Monnier S, Brunel B et al (2021b) Extra-cellular matrix in multicellular aggregates acts as a pressure sensor controlling cell proliferation and motility. *eLife* 10:e63258. <https://doi.org/10.7554/eLife.63258>
- Dzhoyashvili NA, Thompson K, Gorelov AV, Rochev YA (2016) Film thickness determines cell growth and cell sheet detachment from spin-coated poly( N -Isopropylacrylamide) substrates. *ACS Appl Mater Interfaces* 8:27564–27572. <https://doi.org/10.1021/acsami.6b09711>
- Efremov YM, Shpichka AI, Kotova SL, Timashev PS (2019a) Viscoelastic mapping of cells based on fast force volume and PeakForce Tapping. *Soft Matter* 15:5455–5463. <https://doi.org/10.1039/C9SM00711C>
- Efremov YM, Velay-Lizancos M, Weaver CJ et al (2019b) Anisotropy vs isotropy in living cell indentation with AFM. *Sci Rep* 9:5757. <https://doi.org/10.1038/s41598-019-42077-1>
- Efremov YM, Okajima T, Raman A (2020) Measuring viscoelasticity of soft biological samples using atomic force microscopy. *Soft Matter* 16:64–81. <https://doi.org/10.1039/C9SM01020C>
- Efremov Y, Kotova SL, Khlebnikova TM, Timashev PS (2021) A time-shift correction for extraction of viscoelastic parameters from ramp-hold AFM experiments. *Jpn J Appl Phys* 60:SE1002. <https://doi.org/10.35848/1347-4065/abf2d6>
- Engler AJ, Sen S, Sweeney HL, Discher DE (2006) Matrix elasticity directs stem cell lineage specification. *Cell* 126:677–689. <https://doi.org/10.1016/j.cell.2006.06.044>
- Foty RA, Steinberg MS (2005) The differential adhesion hypothesis: a direct evaluation. *Dev Biol* 278:255–263. <https://doi.org/10.1016/j.ydbio.2004.11.012>
- Foty RA, Forgacs G, Pfleger CM, Steinberg MS (1994) Liquid properties of embryonic tissues: measurement of interfacial tensions. *Phys Rev Lett* 72:2298–2301. <https://doi.org/10.1103/PhysRevLett.72.2298>
- Fouchard J, Wyatt TPJ, Proag A et al (2020) Curling of epithelial monolayers reveals coupling between active bending and tissue tension. *Proc Natl Acad Sci U S A* 117:9377–9383. <https://doi.org/10.1073/pnas.1917838117>
- Fujii Y, Ochi Y, Tuchiya M et al (2019) Spontaneous spatial correlation of elastic modulus in jammed epithelial monolayers observed by AFM. *Biophys J* 116:1152–1158. <https://doi.org/10.1016/j.bpj.2019.01.037>
- Fujita A, Ueno K, Saito T et al (2019) Hypoxic-conditioned cardiosphere-derived cell sheet transplantation for chronic myocardial infarction. *Eur J Cardio Thoracic Surg* 56:1062–1074. <https://doi.org/10.1093/ejcts/ezz122>
- Gómez-González M, Latorre E, Arroyo M, Trepat X (2020) Measuring mechanical stress in living tissues. *Nat Rev Phys* 2:300–317. <https://doi.org/10.1038/s42254-020-0184-6>
- Gonçalves AI, Rodrigues MT, Gomes ME (2017) Tissue-engineered magnetic cell sheet patches for advanced strategies in tendon regeneration. *Acta Biomater* 63:110–122. <https://doi.org/10.1016/j.actbio.2017.09.014>
- González-Bermúdez B, Guinea GV, Plaza GR (2019) Advances in micropipette aspiration: applications in cell biomechanics, models, and extended studies. *Biophys J* 116:587–594
- Gonzalez-Rodriguez D, Guevorkian K, Douezan S, Brochard-Wyart F (2012) Soft matter models of developing tissues and tumors. *Science* 30(338):910–917. <https://doi.org/10.1126/science.1226418>
- Goodman TT, Olive PL, Pun SH (2007) Increased nanoparticle penetration in collagenase-treated multicellular spheroids. *Int J Nanomedicine* 2:265–274
- Gorkun AA, Revokatova DP, Zurina IM et al (2021) The duo of osteogenic and angiogenic differentiation in ADSC-derived spheroids. *Front cell Dev Biol* 9:572727. <https://doi.org/10.3389/fcell.2021.572727>
- Graner F, Glazier JA (1992) Simulation of biological cell sorting using a two-dimensional extended Potts model. *Phys Rev Lett* 69:2013–2016. <https://doi.org/10.1103/PhysRevLett.69.2013>
- Grebenik EA, Istranov LP, Istranova EV et al (2019) Chemical cross-linking of xenopericardial biomeshes: a bottom-up study of structural and functional correlations. *Xenotransplantation* 26:e12506. <https://doi.org/10.1111/xen.12506>
- Gryadunova AA, Koudan EV, Rodionov SA et al (2020) Cytoskeleton systems contribute differently to the functional intrinsic properties of chondrospheres. *Acta Biomater* 118:141–152. <https://doi.org/10.1016/j.actbio.2020.10.007>
- Guevorkian K, Maître JL (2017) Micropipette aspiration: a unique tool for exploring cell and tissue mechanics in vivo. *Methods Cell Biol* 139:187–201. <https://doi.org/10.1016/bs.mcb.2016.11.012>
- Guevorkian K, Colbert M-J, Durth M et al (2010) Aspiration of biological viscoelastic drops. *Phys Rev Lett* 104:218101. <https://doi.org/10.1103/PhysRevLett.104.218101>
- Guevorkian K, Gonzalez-Rodriguez D, Carlier C et al (2011) Mechanosensitive shivering of model tissues under controlled aspiration. *Proc Natl Acad Sci U S A* 108:13387–13392. <https://doi.org/10.1073/pnas.1105741108>
- Guillaume L, Rigal L, Fehrenbach J et al (2019) Characterization of the physical properties of tumor-derived spheroids reveals critical insights for pre-clinical studies. *Sci Rep* 9:1–9. <https://doi.org/10.1038/s41598-019-43090-0>
- Guimaraes CF, Gasperini L, Marques AP, Reis RL (2020) The stiffness of living tissues and its implications for tissue engineering. *Nat Rev Mater*. <https://doi.org/10.1038/s41578-019-0169-1>
- Guthold M, Liu W, Sparks EA et al (2007) A comparison of the mechanical and structural properties of fibrin fibers with other protein fibers. *Cell Biochem Biophys* 49:165–181. <https://doi.org/10.1007/s12013-007-9001-4>
- Hammond TG, Hammond JM (2001) Optimized suspension culture: the rotating-wall vessel. *Am J Physiol Physiol* 281:F12–F25. <https://doi.org/10.1152/ajprenal.2001.281.1.F12>
- Harris AK (1976) Is cell sorting caused by differences in the work of intercellular adhesion? A critique of the steinberg hypothesis. *J Theor Biol* 61:267–285. [https://doi.org/10.1016/0022-5193\(76\)90019-9](https://doi.org/10.1016/0022-5193(76)90019-9)
- Harris AR, Peter L, Bellis J et al (2012) Characterizing the mechanics of cultured cell monolayers. *Proc Natl Acad Sci* 109:16449–16454. <https://doi.org/10.1073/pnas.1213301109>

- Harris AR, Bellis J, Khalilgharibi N et al (2013) Generating suspended cell monolayers for mechanobiological studies. *Nat Protoc* 8:2516–2530. <https://doi.org/10.1038/nprot.2013.151>
- Healy D, Nash M, Gorelov A et al (2017a) Nanometer-scale physically adsorbed thermoresponsive films for cell culture. *Int J Polym Mater Polym Biomater* 66:221–234. <https://doi.org/10.1080/00914037.2016.1201765>
- Healy D, Nash M, Gorelov A et al (2017b) An investigation of cell growth and detachment from thermoresponsive physically crosslinked networks. *Colloids Surf B: Biointerfaces* 159:159–165. <https://doi.org/10.1016/j.colsurfb.2017.07.050>
- Hepburn MS, Wijesinghe P, Major LG et al (2020) Three-dimensional imaging of cell and extracellular matrix elasticity using quantitative micro-elastography. *Biomed Opt Express* 11:867. <https://doi.org/10.1364/boe.383419>
- Hoffmann GA, Wong JY, Smith ML (2019) On force and form: mechano-biochemical regulation of extracellular matrix. *Biochemistry* 58:4710–4720. <https://doi.org/10.1021/acs.biochem.9b00219>
- Hsu T-W, Lu Y-J, Lin Y-J et al (2021) Transplantation of 3D MSC/HUVEC spheroids with neuroprotective and proangiogenic potentials ameliorates ischemic stroke brain injury. *Biomaterials* 272:120765. <https://doi.org/10.1016/j.biomaterials.2021.120765>
- Imashiro C, Shimizu T (2021) Fundamental technologies and recent advances of cell-sheet-based tissue engineering. *Int J Mol Sci* 22:425. <https://doi.org/10.3390/ijms22010425>
- Imashiro C, Hirano M, Morikura T et al (2020) Detachment of cell sheets from clinically ubiquitous cell culture vessels by ultrasonic vibration. *Sci Rep* 10:9468. <https://doi.org/10.1038/s41598-020-66375-1>
- Isenberg BC, Backman DE, Kinahan ME et al (2012) Micropatterned cell sheets with defined cell and extracellular matrix orientation exhibit anisotropic mechanical properties. *J Biomech* 45:756–761. <https://doi.org/10.1016/j.jbiomech.2011.11.015>
- Ivascu A, Kubbies M (2006) Rapid generation of single-tumor spheroids for high-throughput cell function and toxicity analysis. *J Biomol Screen* 11:922–932. <https://doi.org/10.1177/1087057106292763>
- Jaiswal D, Cowley N, Bian Z et al (2017) Stiffness analysis of 3D spheroids using microtweezers. *PLoS One* 12:1–21. <https://doi.org/10.1371/journal.pone.0188346>
- Jaiswal D, Moscato Z, Tomizawa Y et al (2019) Elastography of multicellular spheroids using 3D light microscopy. *Biomed Opt Express* 10:2409. <https://doi.org/10.1364/boe.10.002409>
- Janmey PA, Fletcher DA, Reinhart-King CA (2020) Stiffness sensing by cells. *Physiol Rev* 100:695–724. <https://doi.org/10.1152/physrev.00013.2019>
- Jansen KA, Donato DM, Balcioglu HE et al (2015) A guide to mechanobiology: where biology and physics meet. *Biochim Biophys Acta, Mol Cell Res* 1853:3043–3052. <https://doi.org/10.1016/j.bbamer.2015.05.007>
- Jorba I, Uriarte JJ, Campillo N et al (2017) Probing micromechanical properties of the extracellular matrix of soft tissues by atomic force microscopy. *J Cell Physiol* 232:19–26. <https://doi.org/10.1002/jcp.25420>
- Jorgenson AJ, Choi KM, Sicard D et al (2017) TAZ activation drives fibroblast spheroid growth, expression of profibrotic paracrine signals, and context-dependent ECM gene expression. *Am J Phys Cell Phys* 312:C277–C285. <https://doi.org/10.1152/ajpcell.00205.2016>
- Jung W, Li J, Chaudhuri O, Kim T (2020) Nonlinear elastic and inelastic properties of cells. *J Biomech Eng* 142:1–18. <https://doi.org/10.1115/1.4046863>
- Kaiser NJ, Coulombe KLK (2015) Physiologically inspired cardiac scaffolds for tailored in vivo function and heart regeneration. *Biomed Mater* 10:034003. <https://doi.org/10.1088/1748-6041/10/3/034003>
- Kalantarian A, Ninomiya H, Saad SMI et al (2009) Axisymmetric drop shape analysis for estimating the surface tension of cell aggregates by centrifugation. *Biophys J* 96:1606–1616. <https://doi.org/10.1016/j.bpj.2008.10.064>
- Kamao H, Mandai M, Ohashi W et al (2017) Evaluation of the surgical device and procedure for extracellular matrix–scaffold–supported human iPSC–derived retinal pigment epithelium cell sheet transplantation. *Investig Ophthalmology Vis Sci* 58:211. <https://doi.org/10.1167/iovs.16-19778>
- Kasas S, Stupar P, Dietler G (2018) AFM contribution to unveil pro- and eukaryotic cell mechanical properties. *Semin Cell Dev Biol* 73:177–187. <https://doi.org/10.1016/j.semcdcb.2017.08.032>
- Kasza KE, Rowat AC, Liu J et al (2007) The cell as a material. *Curr Opin Cell Biol* 19:101–107. <https://doi.org/10.1016/j.ceb.2006.12.002>
- Khalilgharibi N, Mao Y (2021) To form and function: on the role of basement membrane mechanics in tissue development, homeostasis and disease. *Open Biol* 11:200360. <https://doi.org/10.1098/rsob.200360>
- Khalilgharibi N, Fouchard J, Asadipour N et al (2019) Stress relaxation in epithelial monolayers is controlled by the actomyosin cortex. *Nat Phys* 15:839–847. <https://doi.org/10.1038/s41567-019-0516-6>
- Kim SJ, Jun I, Kim DW et al (2013) Rapid transfer of endothelial cell sheet using a thermosensitive hydrogel and its effect on therapeutic angiogenesis. *Biomacromolecules* 14:4309–4319. <https://doi.org/10.1021/bm4011744>
- Kim M, Yun H-W, Park DY et al (2018) Three-dimensional spheroid culture increases exosome secretion from mesenchymal stem cells. *Tissue Eng Regen Med* 15:427–436. <https://doi.org/10.1007/s13770-018-0139-5>
- Knight E, Przyborski S (2015) Advances in 3D cell culture technologies enabling tissue-like structures to be created in vitro. *J Anat* 227:746–756. <https://doi.org/10.1111/joa.12257>
- Knudsen L, Ochs M (2018) The micromechanics of lung alveoli: structure and function of surfactant and tissue components. *Histochem Cell Biol* 150:661–676
- Kobayashi J, Kikuchi A, Aoyagi T, Okano T (2019a) Cell sheet tissue engineering: cell sheet preparation, harvesting/manipulation, and transplantation. *J Biomed Mater Res Part A* 107:955–967
- Kobayashi Y, Cordonier CEJ, Noda Y et al (2019b) Tailored cell sheet engineering using microstereolithography and electrochemical cell transfer. *Sci Rep* 9:10415. <https://doi.org/10.1038/s41598-019-46801-9>
- Kosheleva NV, Ilina IV, Zurina IM et al (2016) Laser-based technique for controlled damage of mesenchymal cell spheroids: a first step in studying reparation in vitro. *Biol Open* 5:993–1000. <https://doi.org/10.1242/bio.017145>
- Kosheleva NV, Efremov YM, Shavkuta BS et al (2020) Cell spheroid fusion: beyond liquid drops model. *Sci Rep* 10:12614. <https://doi.org/10.1038/s41598-020-69540-8>
- Koudan EV, Gryadunova AA, Karalkin PA et al (2020) Multiparametric analysis of tissue spheroids fabricated from different types of cells. *Biotechnol J* 15:1900217. <https://doi.org/10.1002/biot.201900217>
- Krasina ME, Kosheleva NV, Lipina TV et al (2020) Regenerative potential of a suspension and spheroids of multipotent mesenchymal stromal cells from human umbilical cord on the model of myocardial infarction in rats. *Bull Exp Biol Med* 169:549–557. <https://doi.org/10.1007/s10517-020-04928-0>
- Krieg M, Fläschner G, Alsteens D et al (2019) Atomic force microscopy-based mechanobiology. *Nat Rev Phys* 1:41–57. <https://doi.org/10.1038/s42254-018-0001-7>
- Kumar P, Satyam A, Fan X et al (2015) Macromolecularly crowded in vitro microenvironments accelerate the production of extracellular matrix-rich supramolecular assemblies. *Sci Rep* 5:1–10. <https://doi.org/10.1038/srep08729>
- Kwong G, Marquez HA, Yang C et al (2019) Generation of a purified iPSC-derived smooth muscle-like population for cell sheet engineering. *Stem Cell Reports* 13:499–514. <https://doi.org/10.1016/j.stemcr.2019.07.014>

- Labusca L, Herea DD, Minuti AE et al (2021) Magnetic nanoparticle loaded human adipose derived mesenchymal cells spheroids in levitated culture. *J Biomed Mater Res Part B Appl Biomater* 109:630–642. <https://doi.org/10.1002/jbm.b.34727>
- Larin KV, Sampson DD (2017) Optical coherence elastography – OCT at work in tissue biomechanics. *Biomed Opt Express* 8:1172. <https://doi.org/10.1364/boe.8.001172>
- Lecuit T, Lenne PF (2007) Cell surface mechanics and the control of cell shape, tissue patterns and morphogenesis. *Nat Rev Mol Cell Biol* 8: 633–644. <https://doi.org/10.1038/nrm2222>
- Lee GY, Kenny PA, Lee EH, Bissell MJ (2007) Three-dimensional culture models of normal and malignant breast epithelial cells. *Nat Methods* 4:359–365. <https://doi.org/10.1038/nmeth1015>
- Lekka M, Gil D, Pogoda K et al (2012) Cancer cell detection in tissue sections using AFM. *Arch Biochem Biophys* 518:151–156
- Leroux CE, Palmier J, Boccardo AC et al (2015) Elastography of multicellular aggregates submitted to osmo-mechanical stress. *New J Phys* 17:073035. <https://doi.org/10.1088/1367-2630/17/7/073035>
- Li N, Li X, Chen K et al (2019) Characterization of spontaneous spheroids from oral mucosa-derived cells and their direct comparison with spheroids from skin-derived cells. *Stem Cell Res Ther* 10:184. <https://doi.org/10.1186/s13287-019-1283-0>
- Lin RZ, Chang HY (2008) Recent advances in three-dimensional multicellular spheroid culture for biomedical research. *Biotechnol J* 3: 1172–1184
- Liu J, Kuznetsova LA, Edwards GO et al (2007) Functional three-dimensional HepG2 aggregate cultures generated from an ultrasound trap: comparison with HepG2 spheroids. *J Cell Biochem* 102:1180–1189. <https://doi.org/10.1002/jcb.21345>
- Liu D, Chen S, Win Naing M (2021) A review of manufacturing capabilities of cell spheroid generation technologies and future development. *Biotechnol Bioeng* 118:542–554. <https://doi.org/10.1002/bit.27620>
- Locquet M-A, Dechaume A-L, Berchard P et al (2021) Aldehyde dehydrogenase, a therapeutic target in chordoma: analysis in 3D cellular models. *Cells* 10:399. <https://doi.org/10.3390/cells10020399>
- Magno R, Grieneisen VA, Marée AFM (2015) The biophysical nature of cells: potential cell behaviours revealed by analytical and computational studies of cell surface mechanics. *BMC Biophys*:8
- Mak KM, Mei R (2017) Basement membrane type IV collagen and laminin: an overview of their biology and value as fibrosis biomarkers of liver disease. *Anat Rec* 300:1371–1390. <https://doi.org/10.1002/ar.23567>
- Manning ML, Foty RA, Steinberg MS, Schoetz EM (2010) Coaction of intercellular adhesion and cortical tension specifies tissue surface tension. *Proc Natl Acad Sci U S A* 107:12517–12522. <https://doi.org/10.1073/pnas.1003743107>
- Mazlin V, Xiao P, Dalimier E et al (2018) In vivo high resolution human corneal imaging using full-field optical coherence tomography. *Biomed Opt Express* 9:557. <https://doi.org/10.1364/BOE.9.000557>
- Melo E, Garreta E, Luque T et al (2014) Effects of the decellularization method on the local stiffness of acellular lungs. *Tissue Eng Part C Methods* 20:412–422. <https://doi.org/10.1089/ten.tec.2013.0325>
- Merzouki A, Malaspina O, Chopard B (2016) The mechanical properties of a cell-based numerical model of epithelium. *Soft Matter* 12:4745–4754. <https://doi.org/10.1039/c6sm00106h>
- Millet LJ, Gillette MU (2012) Over a century of neuron culture: from the hanging drop to microfluidic devices. *Yale J Biol Med* 85:501–521
- Mills KL, Garikipati K, Kemkemer R (2011) Experimental characterization of tumor spheroids for studies of the energetics of tumor growth. *Int J Mater Res* 102:889–895. <https://doi.org/10.3139/146.110532>
- Montel F, Delarue M, Elgeti J et al (2011) Stress clamp experiments on multicellular tumor spheroids. *Phys Rev Lett* 107:1–4. <https://doi.org/10.1103/PhysRevLett.107.188102>
- Montel F, Delarue M, Elgeti J et al (2012) Isotropic stress reduces cell proliferation in tumor spheroids. *New J Phys* 14:055008. <https://doi.org/10.1088/1367-2630/14/5/055008>
- Nagase K, Yamato M, Kanazawa H, Okano T (2018) Poly(N-isopropylacrylamide)-based thermo-responsive surfaces provide new types of biomedical applications. *Biomaterials* 153:27–48
- Nahas A, Bauer M, Roux S, Boccardo AC (2013) 3D static elastography at the micrometer scale using Full Field OCT. *Biomed Opt Express* 4: 2138. <https://doi.org/10.1364/boe.4.002138>
- Narasimhan BN, Ting MS, Kollmetz T et al (2020) Mechanical characterization for cellular mechanobiology: current trends and future prospects. *Front Bioeng Biotechnol* 8:1–9. <https://doi.org/10.3389/fbioe.2020.595978>
- Nonaka PN, Uriarte JJ, Campillo N et al (2014) Mechanical properties of mouse lungs along organ decellularization by sodium dodecyl sulfate. *Respir Physiol Neurobiol* 200:1–5. <https://doi.org/10.1016/j.resp.2014.04.008>
- Norotte C, Marga F, Neagu A et al (2008) Experimental evaluation of apparent tissue surface tension based on the exact solution of the Laplace equation. *EPL* 81:46003. <https://doi.org/10.1209/0295-5075/81/46003>
- Norotte C, Marga FS, Niklason LE, Forgacs G (2009) Scaffold-free vascular tissue engineering using bioprinting. *Biomaterials* 30:5910–5917. <https://doi.org/10.1016/j.biomaterials.2009.06.034>
- Okuda A, Horii-Hayashi N, Sasagawa T et al (2017) Bone marrow stromal cell sheets may promote axonal regeneration and functional recovery with suppression of glial scar formation after spinal cord transection injury in rats. *J Neurosurg Spine* 26:388–395. <https://doi.org/10.3171/2016.8.SPINE16250>
- Omelyanenko NP, Karalkin PA, Bulanova EA et al (2020) Extracellular matrix determines biomechanical properties of chondrospheres during their maturation in vitro. *Cartilage* 11:521–531. <https://doi.org/10.1177/1947603518798890>
- Padhi A, Nain AS (2020) ECM in differentiation: a review of matrix structure, composition and mechanical properties. *Ann Biomed Eng* 48:1071–1089. <https://doi.org/10.1007/s10439-019-02337-7>
- Parfenov VA, Petrov SV, Pereira FDAS et al (2020) Scaffold-free, label-free, and nozzle-free magnetic levitational bioassembler for rapid formative biofabrication of 3D tissues and organs. *Int J Bioprinting* 6. <https://doi.org/10.18063/ijb.v6i3.304>
- Patino-Guerrero A, Veldhuizen J, Zhu W et al (2020) Three-dimensional scaffold-free microtissues engineered for cardiac repair. *J Mater Chem B* 8:7571–7590
- Prevedel R, Díz-Muñoz A, Ruocco G, Antonacci G (2019) Brillouin microscopy: an emerging tool for mechanobiology. *Nat Methods* 16:969–977
- Rim NG, Yih A, Hsi P et al (2018) Micropatterned cell sheets as structural building blocks for biomimetic vascular patches. *Biomaterials* 181: 126–139. <https://doi.org/10.1016/j.biomaterials.2018.07.047>
- Roan E, Waters CM (2011) What do we know about mechanical strain in lung alveoli? *Am J Phys Lung Cell Mol Phys* 301:L625–L635
- Roberts EG, PiekarSKI BL, Huang K et al (2019) Evaluation of placental mesenchymal stem cell sheets for myocardial repair and regeneration. *Tissue Eng - Part A* 25:867–877. <https://doi.org/10.1089/ten.tea.2018.0035>
- Ryu H, Park Y, Luan H et al (2021) Transparent, compliant 3D mesostructures for precise evaluation of mechanical characteristics of organoids. *Adv Mater* 2100026. <https://doi.org/10.1002/adma.202100026>
- Schmal O, Seifert J, Schäffer TE et al (2016) Hematopoietic stem and progenitor cell expansion in contact with mesenchymal stromal cells in a hanging drop model uncovers disadvantages of 3D culture. *Stem Cells Int* 2016:1–13. <https://doi.org/10.1155/2016/4148093>
- Shafiee A, Norotte C, Ghadiri E (2017) Cellular bioink surface tension: a tunable biophysical parameter for faster maturation of bioprinted

- tissue. *Bioprinting* 8:13–21. <https://doi.org/10.1016/j.bprint.2017.10.001>
- Shafiee A, Ghadiri E, Ramesh H et al (2019a) Physics of bioprinting. *Appl Phys Rev* 6:021315. <https://doi.org/10.1063/1.5087206>
- Shafiee A, Ghadiri E, Williams D, Atala A (2019b) Physics of cellular self-assembly—a microscopic model and mathematical framework for faster maturation of bioprinted tissues. *Bioprinting* 14:e00047. <https://doi.org/10.1016/j.bprint.2019.e00047>
- Shen H, Cai S, Wu C et al (2021) Recent advances in three-dimensional multicellular spheroid culture and future development. *Micromachines* 12:1–21
- Silva AS, Santos LF, Mendes MC, Mano JF (2020) Multi-layer pre-vascularized magnetic cell sheets for bone regeneration. *Biomaterials* 231:119664. <https://doi.org/10.1016/j.biomaterials.2019.119664>
- Smith A-S (2010) Physics challenged by cells. *Nat Phys* 6:726–729. <https://doi.org/10.1038/nphys1798>
- Solon J, Levental I, Sengupta K et al (2007) Fibroblast adaptation and stiffness matching to soft elastic substrates. *Biophys J* 93:4453–4461. <https://doi.org/10.1529/biophysj.106.101386>
- Sonbol HS (2018) Extracellular matrix remodeling in human disease. *J Microsc Ultrastruct* 6:123. [https://doi.org/10.4103/JMAU.JMAU\\_4\\_18](https://doi.org/10.4103/JMAU.JMAU_4_18)
- Sorba F, Poulin A, Ischer R et al (2019) Integrated elastomer-based device for measuring the mechanics of adherent cell monolayers. *Lab Chip* 19:2138–2146. <https://doi.org/10.1039/c9lc00075e>
- Stamenović D, Smith ML (2020) Tensional homeostasis at different length scales. *Soft Matter* 16:6946–6963. <https://doi.org/10.1039/d0sm00763c>
- Steinberg MS (1963) Reconstruction of tissues by dissociated cells. *Science* 80(141):401–408. <https://doi.org/10.1126/science.141.3579.401>
- Sunyer R, Trepat X, Fredberg JJ et al (2009) The temperature dependence of cell mechanics measured by atomic force microscopy. *Phys Biol* 6:025009. <https://doi.org/10.1088/1478-3975/6/2/025009>
- Swift J, Ivanovska IL, Buxboim A et al (2013) Nuclear lamin-A scales with tissue stiffness and enhances matrix-directed differentiation. *Science* 80(341):1240104. <https://doi.org/10.1126/science.1240104>
- Tang Z, Okano T (2014) Recent development of temperature-responsive surfaces and their application for cell sheet engineering. *Regen Biomater* 1:91–102. <https://doi.org/10.1093/rb/rbu011>
- Tello M, Spenlé C, Hemmerlé J et al (2016) Generating and characterizing the mechanical properties of cell-derived matrices using atomic force microscopy. *Methods* 94:85–100. <https://doi.org/10.1016/jymeth.2015.09.012>
- Tsai AC, Liu Y, Yuan X, Ma T (2015) Compaction, fusion, and functional activation of three-dimensional human mesenchymal stem cell aggregate. *Tissue Eng - Part A* 21:1705–1719. <https://doi.org/10.1089/ten.tea.2014.0314>
- Uesugi K, Akiyama Y, Hoshino T et al (2013) Measuring mechanical properties of cell sheets by a tensile test using a self-attachable fixture. *J Robot Mechatronics* 25:603–610. <https://doi.org/10.20965/jrm.2013.p0603>
- Venugopal B, Shenoy SJ, Mohan S et al (2020) Bioengineered corneal epithelial cell sheet from mesenchymal stem cells—a functional alternative to limbal stem cells for ocular surface reconstruction. *J Biomed Mater Res Part B Appl Biomater* 108:1033–1045. <https://doi.org/10.1002/jbm.b.34455>
- Vogel V (2018) Unraveling the mechanobiology of extracellular matrix. *Annu Rev Physiol* 80:353–387. <https://doi.org/10.1146/annurev-physiol-021317-121312>
- Vyas V, Solomon M, D’Souza GGM, Huey BD (2019) Nanomechanical analysis of extracellular matrix and cells in multicellular spheroids. *Cell Mol Bioeng* 12:203–214. <https://doi.org/10.1007/s12195-019-00577-0>
- Wang J, Liu M, Shen Y et al (2018) Compressive force spectroscopy: from living cells to single proteins. *Int J Mol Sci* 19:960. <https://doi.org/10.3390/ijms19040960>
- Weaver VM, Lelièvre S, Lakins JN et al (2002) beta4 integrin-dependent formation of polarized three-dimensional architecture confers resistance to apoptosis in normal and malignant mammary epithelium. *Cancer Cell* 2:205–216. [https://doi.org/10.1016/s1535-6108\(02\)00125-3](https://doi.org/10.1016/s1535-6108(02)00125-3)
- Wechsler ME, Shevchuk M, Peppas NA (2020) Developing a multidisciplinary approach for engineering stem cell organoids. *Ann Biomed Eng* 48:1895–1904. <https://doi.org/10.1007/s10439-019-02391-1>
- Wenger MPE, Bozec L, Horton MA, Mesquida P (2007) Mechanical properties of collagen fibrils. *Biophys J* 93:1255–1263. <https://doi.org/10.1529/biophysj.106.103192>
- Wu P-H, Aroush DR-B, Asnacios A et al (2018) A comparison of methods to assess cell mechanical properties. *Nat Methods* 15: 491–498. <https://doi.org/10.1038/s41592-018-0015-1>
- Wyatt TPJ, Fouchard J, Lisica A et al (2020) Actomyosin controls planarity and folding of epithelia in response to compression. *Nat Mater* 19:109–117. <https://doi.org/10.1038/s41563-019-0461-x>
- Xi W, Saw TB, Delacour D et al (2019) Material approaches to active tissue mechanics. *Nat Rev Mater* 4:23–44. <https://doi.org/10.1038/s41578-018-0066-z>
- Yang M, Kang E, Wook SJ, Hong J (2017) Surface engineering for mechanical enhancement of cell sheet by nano-coatings. *Sci Rep* 7:4464. <https://doi.org/10.1038/s41598-017-04746-x>
- Yang J, Pan X, Wang L, Yu G (2020) Alveolar cells under mechanical stressed niche: critical contributors to pulmonary fibrosis. *Mol Med* 26:95
- Yoshikawa Y, Miyagawa S, Toda K et al (2018) Myocardial regenerative therapy using a scaffold-free skeletal-muscle-derived cell sheet in patients with dilated cardiomyopathy even under a left ventricular assist device: a safety and feasibility study. *Surg Today* 48:200–210. <https://doi.org/10.1007/s00595-017-1571-1>
- You Q, Liu Z, Zhang J et al (2020) Human amniotic mesenchymal stem cell sheets encapsulating cartilage particles facilitate repair of rabbit osteochondral defects. *Am J Sports Med* 48:599–611. <https://doi.org/10.1177/0363546519897912>
- Young RE, Graf J, Miserocchi I et al (2019) Optimizing the alignment of thermoresponsive poly(N-isopropyl acrylamide) electrospun nanofibers for tissue engineering applications: a factorial design of experiments approach. *PLoS One* 14:e0219254. <https://doi.org/10.1371/journal.pone.0219254>
- Yu M, Mahtabfar A, Beelen P, Demiryurek Y, Shreiber DI, Zahn JD, Foty RA, Liu L, Lin H (2018) Coherent timescales and mechanical structure of multicellular aggregates. *Biophys J* 114:2703–2716. <https://doi.org/10.1016/j.bpj.2018.04.025>
- Yurchenco PD (2011) Basement membranes: cell scaffoldings and signaling platforms. *Cold Spring Harb Perspect Biol* 3:a004911–a004911. <https://doi.org/10.1101/cshperspect.a004911>
- Zaitsev VY, Matveyev AL, Matveev LA et al (2021) Strain and elasticity imaging in compression optical coherence elastography: the two-decade perspective and recent advances. *J Biophotonics* 14. <https://doi.org/10.1002/jbio.202000257>
- Zhang W, Wang S, Lin M et al (2012) Advances in experimental approaches for investigating cell aggregate mechanics. *Acta Mech Solida Sin* 25:473–482. [https://doi.org/10.1016/S0894-9166\(12\)60042-1](https://doi.org/10.1016/S0894-9166(12)60042-1)
- Zhang S, Liu P, Chen L et al (2015) The effects of spheroid formation of adipose-derived stem cells in a microgravity bioreactor on stemness properties and therapeutic potential. *Biomaterials* 41:15–25. <https://doi.org/10.1016/j.biomaterials.2014.11.019>
- Zhang K, Zhu M, Thomas E et al (2021) Existing and potential applications of elastography for measuring the viscoelasticity of biological

- tissues *in vivo*. Front Phys 9:13–16. <https://doi.org/10.3389/fphy.2021.670571>
- Zhu Y, Thakore AD, Farry JM et al (2021) Collagen-supplemented incubation rapidly augments mechanical property of fibroblast cell sheets. *Tissue Eng Part A* 27:328–335. <https://doi.org/10.1089/ten.tea.2020.0128>
- Zollinger AJ, Xu H, Figueiredo J et al (2018) Dependence of tensional homeostasis on cell type and on cell–cell interactions. *Cell Mol Bioeng* 11:175–184
- Zurina IM, Shpichka AI, Saburina IN et al (2018) 2D/3D buccal epithelial cell self-assembling as a tool for cell phenotype maintenance and fabrication of multilayered epithelial linings *in vitro*. *Biomed Mater* 13:054104. <https://doi.org/10.1088/1748-605X/aace1c>
- Zurina IM, Gorkun AA, Dzhussoeva EV et al (2020a) Human melanocyte-derived spheroids: a precise test system for drug screening and a multicellular unit for tissue engineering. *Front Bioeng Biotechnol* 8:540. <https://doi.org/10.3389/fbioe.2020.00540>
- Zurina IM, Presniakova VS, Butnaru DV et al (2020b) Tissue engineering using a combined cell sheet technology and scaffolding approach. *Acta Biomater* 113:63–83

**Publisher's note** Springer Nature remains neutral with regard to jurisdictional claims in published maps and institutional affiliations.